

## Changes in Axon Fluorescence during Activity: Molecular Probes of Membrane Potential

L. B. Cohen, B. M. Salzberg, H. V. Davila\*, W. N. Ross,  
D. Landowne\*\*, A. S. Waggoner, and C. H. Wang

Department of Physiology, Yale University School of Medicine,  
New Haven, Connecticut 06510,  
Department of Chemistry, Amherst College, Amherst, Massachusetts, and  
The Marine Biological Laboratory, Woods Hole, Massachusetts

Received 11 February 1974

*Summary.* The fluorescence of dyes added to squid giant axons was studied during action potentials and voltage-clamp steps. One goal was to find fluorescence changes related to the increases in membrane conductance that underlie propagation. A second goal was to find large changes in fluorescence that would allow optical monitoring of membrane potential in neurons and other cells. Attempts were made to measure fluorescence changes using over 300 different fluorescent molecules and positive results were obtained with more than half of these. No evidence was found that would relate any of the fluorescence changes to the increases in membrane conductance that accompany depolarization; most, instead, were correlated with the changes in membrane potential. The fluorescence changes of several dyes were relatively large; the largest changes during an action potential were  $10^{-3}$  of the resting intensity. They could be measured with a signal-to-noise ratio of better than 10:1 in a single sweep.

Changes in the fluorescence of molecules added to axons have been studied in an effort to learn about alterations in membrane structure that occur during excitation (Tasaki, Carnay & Watanabe, 1969; Cohen, Landowne, Shrivastav & Ritchie, 1970; Conti, Tasaki & Wanke, 1971). Although it was suggested that ANS and TNS fluorescence changes were related to increases in membrane conductance, our experiments (Davila, Cohen, Salzberg & Shrivastav, 1974) indicated that these fluorescence changes were, in fact, potential dependent. With the hope that other dyes would provide information about the structural basis of the conductance

---

\* *Present address:* Departamento de Fisiologia, Facultad de Medicina, Universidad Los Andes, Merida, Venezuela.

\*\* *Present address:* Department of Physiology and Biophysics, University of Miami School of Medicine, Miami, Florida.

increases that underlie the action potential, we began a survey of fluorescent molecules.

This survey had another objective; we wished to find a molecule with a large change in fluorescence. Such a probe could provide a powerful technique for measuring membrane potential in systems where, for reasons of scale, topology, or complexity, the use of electrodes would be inconvenient or impossible. Because of this objective, most of our experiments were carried out with dyes added to the external bathing solution.

Preliminary reports of these experiments have been published (Cohen *et al.*, 1970; Cohen, Davila & Waggoner, 1971; Salzberg, Davila, Cohen & Waggoner, 1972; Cohen, 1973; Davila, Salzberg, Cohen & Waggoner, 1973), and the techniques have been demonstrated (Cohen, Salzberg & Davila, 1973).

### Materials and Methods

Giant axons with diameters of 330 to 820  $\mu\text{m}$  were dissected from the hindmost stellar nerves of the squid, *Loligo pealii*, and cleaned of small fibers. In a few experiments, walking leg nerves from the lobster, *Homarus americanus*, were used; these were obtained by the pulling-out method of Furusawa (1929).

The apparatus used for measuring fluorescence changes in giant axons is shown schematically in Fig. 1. For most dyes, the light source was a quartz-halogen tungsten-filament lamp. Interference filters of 30-nm width at half-height (Oriel Optics Corp.) were used to provide the incident excitation light of appropriate wavelengths (filter 1). The wavelength of peak transmittance of the filter is the number in column three of Table 3. The secondary filters (filter 2) were Schott, long-wavelength-pass filters chosen to block the excitation wavelengths but to pass as much as possible of the emitted light. The current output from the silicon photodiode detector (E.G. & G, SGD 444) was converted to voltage with a Philbrick Q25AH operational amplifier used in a current-measuring configuration. This voltage was further amplified with a Tektronix 3A9 amplifier with a low-pass filter and the resulting signal stored in a signal averager in order to improve the signal-to-noise ratio. After an appropriate number of traces the averaged signal was written out on an X-Y recorder. Further details of the apparatus are given in the legend of Fig. 1 and in Davila *et al.* (1974).

In most experiments the dye solution (usually 0.01 to 0.1 mg/ml dye in sea water) was incubated with the axon for 10 min. The dye solution was then replaced with sea water that had been bubbled with nitrogen gas. The deoxygenation effectively eliminated the photodynamic damage to the axon (Arvanitaki & Chalazonitis, 1961; Pooler, 1972) that would have occurred with some dyes. With dyes that were only slightly soluble in sea water, Pluronic F-127 (BASF Wyandotte Corp., Wyandotte, Michigan), a high molecular-weight surfactant polyol, was included in the dye solution, using the following procedure. An ethanol solution of the dye was added to melted (55 °C) Pluronic. Hot (55 °C) sea water was then added in sufficient amounts to give a final concentration of 1% ethanol and the desired concentration of dye. The solution was cooled to  $\leq 30$  °C and then added to the axon. The actual ethanol concentration was less than 1% because of evaporation during addition to melted Pluronic. The final Pluronic concentration was limited to the range 0.01 to 0.2%; Pluronic concentrations in excess of 0.2% led to spontaneous firing of the axon. The chamber was maintained at constant temperatures between 9 and 15 °C, unless otherwise specified.

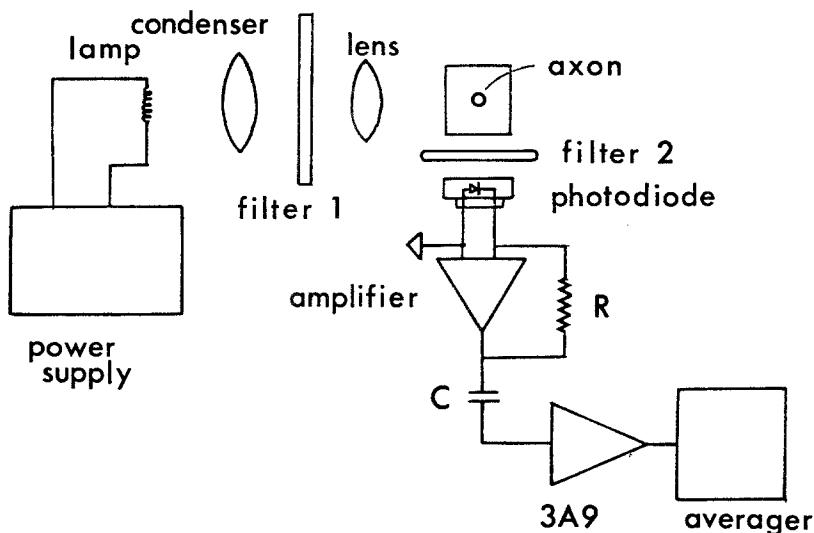


Fig. 1. Schematic drawing of apparatus used to measure fluorescence changes in axons. The light source was a 100 W quartz-halogen tungsten-filament lamp in a Schoeffel LH 150 Lamp housing. The lamp was powered by a Kepco JQE 75-15 (M) HS power supply (KEPCO, Inc., Flushing, N.Y.) operated in the constant voltage mode. The output of the lamp was focused onto a 5 mm length of axon by the condenser and a second quartz lens. The incident radiant flux density (intensity) at the axon was  $0.1 \text{ watts/cm}^2$  with filter 1 of  $570 \pm 15 \text{ nm}$ . Between the two lenses were two heat filters (G-776-7100, Oriel Optics Corp., Stamford, Conn.) and an interference filter, filter 1 (Oriel Optics Corp., Stamford, Conn.). The barrier filters (filter 2) were made by Schott Optical Glass, Inc., Duryea, Pa. The photodiode was an SGD 444 (E.G. & G., Inc., Salem, Mass.) and the amplifier used to convert current to voltage was a battery powered Q25AH operational amplifier (Philbrick Researches, Inc., Dedham, Mass.). Additional amplification and high frequency filtration was provided by a Tektronix 3A9. The output of the 3A9 amplifier was fed into one of two signal averagers, a Biomac 1000 (Data Laboratories, Ltd., Mitchum, Surrey, England), or a TDH-9 waveform eductor (Princeton Applied Research Corp., Princeton, N.J.)

The electrodes and amplifiers used for voltage-clamp experiments were the same as previously described (Cohen, Keynes & Landowne, 1972a; Davila *et al.*, 1974) and compensation for the resistance in series with the membrane was used (Davila *et al.*, 1974). Dyes added to the inside of the axon membrane were microinjected into the axoplasm using the technique of Hodgkin and Keynes (Keynes, 1963).

The absorption spectra of the dye solutions presented in Table 5 were obtained with a Cary 15 spectrometer. Emission spectra were obtained with a Perkin Elmer MPF 3 spectrofluorimeter equipped with an R446F photomultiplier tube. The wavelengths of maximum emission quoted in Table 5 were not corrected for instrument sensitivity. However, the relative intensities of the emission peaks were corrected for variations in lamp intensity with wavelength and for monochromator and photomultiplier characteristics. A rhodamine B photon counter and an E.G. & G. standard lamp were used to obtain the correction factors. The optical density of all fluorescence samples was kept below 0.05 at the exciting wavelength. The samples were deoxygenated by bubbling with nitrogen for several minutes before sealing the cuvette. Where absorption

Table 1. Dye sources

---

A.	Chroma-Gesellschaft Schmid & Co.
B.	Fisher Scientific Co.
C.	MC & B Manufacturing Chemists
D.	Allied Chemical Corp.
E.	George T. Gurr, Ltd.
F.	K. & K. Laboratories, Inc.
G.	Eastman Research Laboratories
H.	synthesized for these experiments
I.	Harleco
J.	E. I. DuPont DeNemours & Co., Inc.
K.	Calbiochem
L.	Aldrich Chemical Co., Inc.
M.	Eastman Kodak, Co.
N.	L. B. Holliday & Co., Ltd.
O.	Intracolor Corp.
P.	BASF Wyandotte Corp.
Q.	AGFA-Gevaert AG
R.	Sigma Chemical Co.
S.	Merck and Co., Inc.
T.	Nutritional Biochemicals Corp.
U.	Sandoz Colors and Chemicals
V.	Imperial Chemical Industries, Ltd.
W.	Edward Gurr, Ltd.
X.	Dr. L. Stryer
Y.	Dr. B. Chance
NK.	Nippon Kankoh-Shikiso Kenkyusho Co., Ltd.

---

and emission maxima were close, as in the merocyanine and cyanine dyes, the dyes were excited on the short wavelength shoulder of the absorption spectrum.

The sources of supply of the dyes are listed in Table 1. The letter in column two of Table 2 and the letters in parentheses in the Appendix refer to the letter and source given in Table 1. The synthetic procedures used for making several dyes labeled with the letter H are given below. Several of the dyes were gifts of Eastman Research Laboratories. Dye I can be purchased as "merocyanine 540" from Eastman Kodak Co.

### *Thin-Layer Chromatography*

Since many of the commercially available dyes we studied were known to be impure (Dobres & Moats, 1968; Dunnigan, 1968; Lillie, 1969, p. 11; Löhr & Wittekind, 1973), we examined each of the trinuclear-heterocyclic dyes and several cyanine, merocyanine and styryl dyes using thin-layer chromatography. Gelman instant thin-layer chromatography medium (Type SG) was used in a Gelman (51325) chamber. The solvent systems most often used were chloroform-methanol mixtures, but, in a few instances higher alcohols were employed.

The trinuclear-heterocyclic dyes generally contained several fluorescent components. The oxazines and acridines seemed to be especially bad in this regard; often we were able to separate more than five components. In addition, there seemed to be

some confusion in the labeling of these dyes. For instance, the major fluorescent component of neutral violet (17) (I) had the same chromatographic and spectrophotometric characteristics as the major component of neutral red (13) (B, C). Therefore, it is possible, or likely in the case of neutral violet, that in some instances a fluorescence change is incorrectly attributed to the major component when it actually results from some fluorescent impurity. Obviously, any interpretation of the fluorescence changes of the trinuclear-heterocyclic dyes in terms of structure will have to be made cautiously. On the other hand, the cyanine, merocyanine and styryl dyes seemed to be relatively pure; in most cases more than 95 % of the dye in these samples traveled in one (or two) bands. Where two bands were found, they had the same color and fluorescence; we suppose that they were cis-trans isomers of the same compound. The dyes that were synthesized for these experiments had only trace contaminants.

### *Synthesis of Merocyanine and Cyanine Dyes*

The merocyanine dyes were prepared according to the procedures described by Brooker, Keyes, Sprague, Van Dyke, Van Lare, Van Zandt, White, Cressman and Dent (1951). The melting points are uncorrected. The quarternary salts (QS), keto-methylenes (KM), and other intermediates are listed below:

- QS 1. Anhydro-2-(4-methoxy-1,3-butadienyl)-3-( $\gamma$ -sulfopropyl)-benzoxazolium hydroxide.
- QS 2. Anhydro-2-(4-methoxy-1,3-butadienyl)-3-( $\gamma$ -sulfopropyl)-benzothiazolium hydroxide.
- QS 3. Anhydro-2-(4-acetanilido-1,3-butadienyl)-1-( $\gamma$ -sulfopropyl)-3,3-dimethyl pseudindolium hydroxide.
- QS 4. Anhydro-2-(4-acetanilido-1,3-butadienyl)-3-( $\gamma$ -sulfopropyl)-2-thiazolinium hydroxide.
- QS 5. 2-(4-methoxy-1,3-butadienyl)-3-( $\beta$ -carboxyethyl)-benzoxazolium bromide.
- QS 6. 2-(4-methoxy-1,3-butadienyl)-3-ethylbenzoxazolium iodide.
- QS 7. 2-(4-methoxy-1,3-butadienyl)-3-( $\gamma$ -bromopropyl)-benzoxazolium bromide.
- QS 8. Anhydro-2-methyl-3-( $\gamma$ -sulfopropyl)-benzoxazolium hydroxide.
- KM 1. 1,3-diethyl-2-thiobarbituric acid.
- KM 2. 1,3-dibutyl-2-thiobarbituric acid.
- KM 3. 1,3-dibutylbarbituric acid.
- R 1. 5-(5-acetanilido-2,4-pentadienylidene)-1,3-diethyl-2-thiobarbituric acid.

The purity of the dyes was confirmed by their spectroscopic properties and thin-layer chromatography using Eastman Chromagram sheet developed with acetone. A summary of the synthetic procedures is listed in Table 2. The details of the preparation of one typical merocyanine dye (IX), one cyanine dye, 3,3'-dihexyloxacarbocyanine (V) and anthroyl TEA are described below.

### *5-[(3,3-Dimethyl-1- $\gamma$ -Sodium-Sulfopropyl-2(3H)-Indolylidene)-2-Butenylidene]-1,3-Dibutyl-2-Thiobarbituric Acid (IX)*

The 2,3,3-trimethyl indolenine (0.8 g, 5 mmoles) and 3-propane sultone (0.7 g, 5 mmoles) were heated at 100 °C for 1 hr. The resulting redish solid was cooled and washed several times with ether. The  $\beta$ -anilidoacrolein anil hydrochloride (1.3 g,

Table 2. Summary of the dye syntheses

Dye No.	Reactants <sup>a</sup>	Me- dium <sup>i</sup>	Base <sup>b</sup>	Re- fluxed min	Rec. solvent	Mp(°C) <sup>g</sup>	$\lambda_{\text{MAX}}^{\text{ABS}}$ <sup>h</sup> (nm)	$\lambda_{\text{MAX}}^{\text{FL}}$ <sup>h</sup> (nm)
IX	QS 3, KM 2	EtOH	Et <sub>3</sub> N	30	acetone	190–195 <sup>c</sup>	591	612
X	QS 5, KM 2	EtOH	Et <sub>3</sub> N	30	EtOH	257–260	559	581
XI	QS 5, KM 1	EtOH	Et <sub>3</sub> N	30	EtOH	> 360	558	581
XII	QS 6, KM 1	EtOH	Et <sub>3</sub> N	30	acetone	254	558	580
XIII	QS 7, KM 1	EtOH	Pyr. <sup>j</sup>	20	DMF/ether	278–280	563	586
XIV	QS 8, R 1	AC <sub>2</sub> O	AcONa	60	EtOH	> 360 <sup>d</sup>	633	664
XV	QS 2, KM 2	EtOH	Et <sub>3</sub> N	30	EtOH	280–285 <sup>e</sup>	593	615
XVI	QS 3, KM 3	EtOH	Et <sub>3</sub> N	30	EtOH	288–289	567	589
III	QS 4, KM 2	EtOH	Et <sub>3</sub> N	30	acetone	250–253 <sup>f</sup>	541	567

<sup>a</sup> Usually 5 to 10 mmoles each. <sup>b</sup> About 5 % in excess. <sup>c</sup> Softens at 160 °C. <sup>d</sup> Decomposed at 300 °C. <sup>e</sup> Softens at 250 °C. <sup>f</sup> Softens at 230 °C. <sup>g</sup> All dyes melted with decomposition.

<sup>h</sup> Error limit ca.  $\pm 1$  nm in EtOH. <sup>i</sup> 15 ml per 5 mmoles each of the reactions. <sup>j</sup> Converted to trimethylamine salt by reflux in 25 % trimethylamine solution overnight.

5 mmoles) and 15 ml of acetic anhydride were added. The mixture was heated on a steam bath for 30 min and the precipitate rinsed several times with ether. The resulting crude anhydro-2-(4-acetanilido-1,3-butadienyl)-1-( $\gamma$ -sulfopropyl)-3,3-dimethyl pseudo-indolium hydroxide (QS4) was used without further purification.

To the crude QS4 was added 1.25 g (5 mmoles) of 1,3-dibutyl-2-thiobarbituric acid (KM2), 20 ml of absolute ethanol and 5 ml (excess) of triethylamine. The whole mixture was refluxed for 30 min and cooled. After evaporating most of the solvent, the residue dye solution, which contained mostly the dye (IX), contaminated with some oxonol and dicarbocyanine, was run through a silica gel column and eluted with acetone. The purified dye was converted to the sodium salt by dissolving the solid in a hot saturated solution of sodium iodide in methanol and collecting the crystals after cooling. The dye was recrystallized from acetone to give 1 g of pure dye, mp 190 to 195 °C (softens at 160 °C).

### 3,3'-Dihexyloxacarbocyanine (V)

The 2-methylbenzoxazole (8 g, 50 mmoles) and *n*-hexyl iodide were heated together at 130 °C for 48 hr. The resulting brown oil was treated with pyridine. The crystals that appeared were collected and rinsed thoroughly with ether, yield 17 g. The crude 3-hexyl-2-methyl benzoxazolium iodide was used without further treatment.

The crude 3-hexyl-2-methyloxazolium iodide (10 g, 28 mmoles) and 12 g (excess) of triethyl orthoformate were heated to reflux with 30 ml of pyridine for 10 hr. The resulting dark brown solution was diluted with 10 ml of methanol and 20 ml of ether and set aside to crystalize. The solid was collected and recrystallized twice from either ethanol or acetone, yield 4.2 g, mp 221 to 222 °C.

The dye can also be prepared from the corresponding *p*-chlorobenzene sulfonate and converted to the iodide at the final stage by crystalizing from a hot water solution containing potassium iodide, as described by Czikkely, Dreizler, Försterling, Kuhn, Sondermann, Tillmann and Wiegand (1969).

*Anthroyl-TEA**3-(9-Anthroyl)-propyl Triethyl Ammonium Iodide*

3-Chloro-1-propanol was reacted with anthracene-9-carboxylic acid chloride in dry benzene for 24 hr with refluxing. The cooled reaction mixture was washed with aqueous  $\text{NaHCO}_3$ , dried, and the benzene removed. The product, 3-(9-anthroyl)-1-iodopropane, was refluxed with sodium iodide in methyl-ethyl ketone for 24 hr; the  $\text{NaCl}$  salt was removed, and the product isolated. This compound was reacted with three equivalents of triethyl amine in ethanol. The precipitated light yellow final product was collected. The anthroyl-TEA-6C (252) was synthesized by a similar procedure.

**Results**

Fig. 2 illustrates the simultaneous measurement of fluorescence (heavy line) and potential (thin line) in a giant axon from *Loligo* that had been stained with a merocyanine dye (I). (Roman numerals refer to dyes in Tables 3 and 4, Arabic numerals refer to dyes listed in the Appendix.) There was an obvious increase in fluorescence intensity at the time of the action potential. Several control experiments indicated that these intensity changes were not artifacts: no intensity changes were measured in axons that were not stained; intensity changes could only be measured when the wavelength of the incident light was near the absorption maximum of the dye; and, finally, removal of the secondary filter (filter 2) gave rise to intensity changes

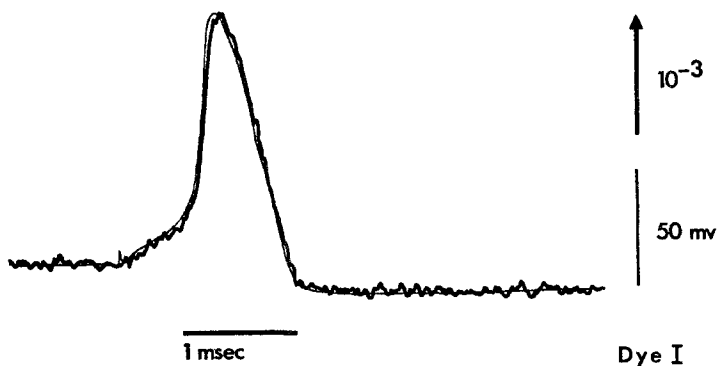


Fig. 2. Fluorescence change of dye I during membrane action potentials. The heavy trace is the record of fluorescence intensity and the light trace is the membrane potential, recorded simultaneously. In this, and in subsequent figures, the direction of the vertical arrow to the right of the tracings indicates the direction of an increase in intensity, and the size of the arrow represents the stated value of the change in intensity  $\Delta I$  divided by the resting intensity  $I_r$  for a single sweep. All records are traced from the originals. The excitation wavelength was  $570 \pm 15$  nm, and filter 2 was a Schott RG 610. The response time constant of the light measuring system was  $35 \mu\text{sec}$ ; 16 sweeps averaged. Temperature  $15^\circ\text{C}$

characteristic of light-scattering effects (Cohen *et al.*, 1972*a, b*) which were very different from the fluorescence changes discussed here.

It was clear from the result shown in Fig. 2 that the time course of this fluorescence increase was very similar to the time course of the potential change during the spike. The very small delay of the fluorescence with respect to potential shown in Fig. 2 resulted primarily from the 35- $\mu$ sec response time-constant of the light-measuring system. The fluorescence increase and the potential change, therefore, had time courses that were remarkably similar. Since the currents and conductance changes that occur during the action potential do not have precisely the same time course as the potential (Cole & Curtis, 1939; Hodgkin & Huxley, 1952), the result in Fig. 2 suggests that fluorescence was in some way dependent on membrane potential rather than on current or conductance. To distinguish more clearly among changes dependent on potential, conductance and current, fluorescence was measured during voltage-clamp steps.

The top three traces in Fig. 3 show such an experiment with the same merocyanine dye (I). During the hyperpolarizing step, on the left, the ionic currents were very small and there was no appreciable conductance change; only the membrane potential varied. There was, however, a fluorescence decrease during this hyperpolarizing step, and it had a time course similar to that of the potential; this fluorescence change therefore depended on membrane potential and not on ionic current or membrane conductance. During the depolarizing step, on the right, there were large currents and conductance increases, but the fluorescence increase had the size and time course expected from the decrease during the hyperpolarizing step on the assumption that the fluorescence of dye I varied linearly with membrane potential. The fluorescence increase during the depolarizing step could not be correlated with the ionic currents or membrane conductance.

Similar experiments were carried out with each of the 320 dyes we have surveyed. With the exception of malachite green and anthroyl stearic acid (*see below*), all of the fluorescence changes had time courses that were similar for hyperpolarizing and depolarizing potential steps, and, thus, they seemed to be potential dependent. However, not all of the changes could be measured with a large enough signal-to-noise ratio (in a reasonable number of sweeps) to be sure about the similarity of time courses. The record for dye I (Fig. 3, top trace) was among the best that we achieved, while that for neutral violet (17) (Fig. 3, bottom trace) was considered to be just satisfactory; no decision could be reached with dyes whose averaged records had smaller signal-to-noise ratios. In addition, if the axon were in poor condition, having small currents and conductance increases, then the



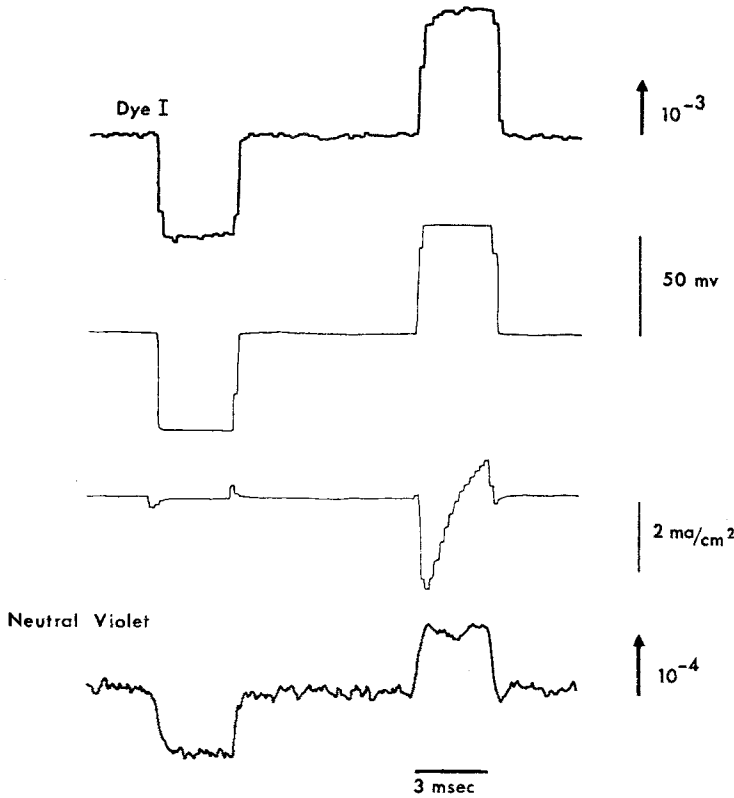


Fig. 3. Fluorescence changes of dye I (top trace) and neutral violet (17) (bottom trace) during hyperpolarizing and depolarizing potential steps (second trace). The fluorescence changes had the same shape as the potential and were unaffected by the large currents (third trace) and conductance changes that occurred during the depolarizing step. The current density and potential records were from the experiment with dye I. The peak inward current during the depolarizing step was  $2.7 \text{ mA/cm}^2$  in the neutral violet experiment. In this, and in subsequent figures, the holding potential was the resting potential, hyperpolarizing is represented downward, inward current is downward. The neutral violet concentration in the external sea water during the experiment was  $5 \mu\text{M}$ . Excitation wavelengths were  $570 \pm 15 \text{ nm}$  and  $540 \pm 15 \text{ nm}$  and barrier filters (filter 2) were Schott RG 610 and OG 590 for dye I and neutral violet, respectively. 25 sweeps were averaged for the experiment with dye I; 4,000 for the neutral violet experiment. The response time constants of the light measuring system were  $70 \mu\text{sec}$  and  $380 \mu\text{sec}$ . Temperature  $12^\circ\text{C}$ .

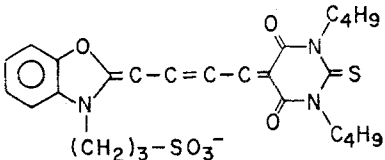
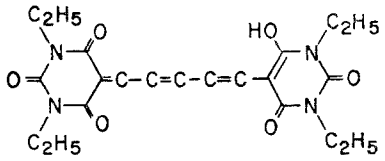
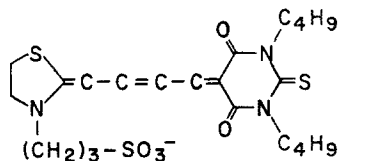
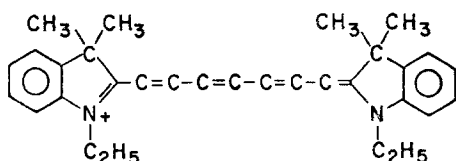
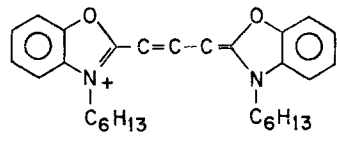
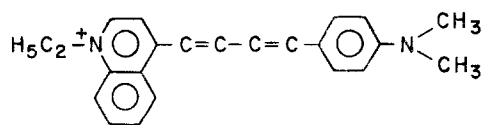
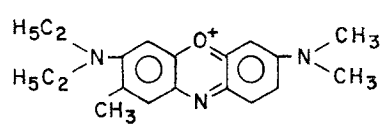
fluorescence change would almost certainly appear to be potential dependent. For this reason, we determined that the fluorescence change of a given dye was potential dependent and unrelated to current or conductance only if the peak inward current density during a 50-mV depolarizing step was greater than  $1.3 \text{ mA/cm}^2$ . (An axon with this inward current density will generate an action potential of about 90 to 95 mV.) Using these criteria,

each of the fluorescence changes given in Tables 3 and 4 (except for XII) were determined to be potential dependent, as were most of the larger changes listed in the Appendix. There was no evidence that would relate any of the fluorescence changes to membrane conductance.

Because voltage-clamp experiments allowed a decision to be made about the potential dependence of the fluorescence changes, this kind of experiment was routinely used in our survey of dyes. For each such experiment, we calculated the signal-to-noise ratio for a single sweep with a 50-mV step, normalizing to a response time constant of 250  $\mu$ sec in the light-measuring system. The size of the fluorescence change was measured at the end of a 3-msec step and the value for the noise was taken to be the second largest peak-to-peak noise excursion in any 1-msec time interval in the 20-msec trace. The signal-to-noise ratios for several dyes which gave large signals are shown in the fifth column of Table 3. As indicated in Table 3, we found large changes in fluorescence using dyes of several types, including merocyanines (I, III), oxonols (II), cyanines (IV, V), styryls (VI) and oxazines (VII). Table 3 also shows that the optimum incident wavelength ranged from 480 nm to at least 690 nm. The wavelength for dye IV is in parentheses because it was not possible to test longer wavelengths with available filters. From its absorption spectrum we expect that the best wavelength for dye IV will be about 740 nm. The nonamethine derivative of dye IV would have an excitation maximum shifted further into the infrared. The largest signal-to-noise ratio found with a dye absorbing at shorter wavelengths was 0.2 for ANS (280), whose excitation maximum was 375 nm. The signal-to-noise ratio shown in each case is the average obtained using the optimum dye concentration and excitation wavelength. There was variability from axon to axon; the average signal-to-noise ratio in eleven experiments with dye I was  $5.3 \pm 0.6$  (standard error of the mean). In addition, the change in intensity  $\Delta I$  divided by the resting intensity  $I_r$  in a single sweep was calculated for a 50-mV depolarizing step. These values are given in column 4 of Table 3.

While the  $\Delta I/I_r$  sweep should be independent of the experimental apparatus, this will not be true of the signal-to-noise ratio. With a large resting fluorescence, the noise in the measurements was predominantly due to random arrival of photons at the photodetector, and the signal-to-noise ratio was proportional to  $(I_r)^{1/2}$  (Braddick, 1960). In this situation the signal-to-noise ratio depended upon the incident excitation intensity, the fraction of the emitted light reaching the detector, the quantum efficiency of the detector, as well as  $\Delta I/I_r$  (Cohen, Hille & Keynes, 1969). With lower light levels the detector and amplifier noise reduced the signal-to-noise

Table 3. Dyes with relatively large changes in fluorescence

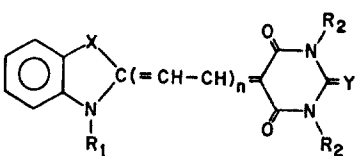
	Source	Excitation wavelength (nm)	$\Delta I/I_r \times 10^4$	S/N
I 	M	570	+7	5
II 	M	600	+1	0.8
III 	H	540	+5	3
IV 	NK	(690)	+3	4
V 	H	480	+1	1
VI 	NK	570	+2	2
VII 	A	600	+2	1

ratio below that predicted from  $\Delta I/I_r$  and  $(I_r)^{1/2}$ . Even though the signal-to-noise ratio is, therefore, dependent upon the particular apparatus used in the measurement, it does provide an indication of which fluorescent molecules would be most useful for monitoring changes in membrane potential.

### *Relationships between Signal Size and Dye Structure*

One factor limiting the use of fluorescence as a monitor of membrane potential is signal size. Although preliminary results already indicate that several of the dyes in Table 3 will provide easily measured signals when used with preparations where fluorescence can be measured from a large amount of membrane (*see* Discussion), signal averaging would be needed to achieve adequate signal size and good time resolution in the experiments on more typical neurons. In an effort to find larger signals and to learn which parts of the fluorescent molecules were important, several analogues of commercially available dyes were synthesized. Table 3, which is intended primarily to indicate dyes which show promise as probes of potential, suggests that the indocyanines give larger signals than the oxacyanines (IV and V, and Appendix); we therefore synthesized an indocyanine derivative of dye I. As indicated in Table 4, this variation (IX) did result in a

Table 4. Simple substituent analogues of dye I

						
Dye	X	R <sub>1</sub>	n	R <sub>2</sub>	Y	S/N
I	O	(CH <sub>2</sub> ) <sub>3</sub> SO <sub>3</sub> <sup>-</sup>	2	C <sub>4</sub> H <sub>9</sub>	S	5
IX	H <sub>3</sub> C—C—CH <sub>3</sub>	(CH <sub>2</sub> ) <sub>3</sub> SO <sub>3</sub> <sup>-</sup>	2	C <sub>4</sub> H <sub>9</sub>	S	8
X	O	(CH <sub>2</sub> ) <sub>2</sub> COO <sup>-</sup>	2	C <sub>4</sub> H <sub>9</sub>	S	2
XI	O	(CH <sub>2</sub> ) <sub>3</sub> SO <sub>3</sub> <sup>-</sup>	2	C <sub>2</sub> H <sub>5</sub>	S	1
XII	O	C <sub>2</sub> H <sub>5</sub>	2	C <sub>2</sub> H <sub>5</sub>	S	0.02
XIII	O	$\begin{array}{c} (\text{CH}_2)_3 \\   \\ \text{H}_3\text{C}-\text{N}^+-\text{CH}_3 \\   \\ \text{CH}_3 \end{array}$	2	C <sub>2</sub> H <sub>5</sub>	S	0.1
XIV	O	(CH <sub>2</sub> ) <sub>3</sub> SO <sub>3</sub> <sup>-</sup>	3	C <sub>2</sub> H <sub>5</sub>	S	1
XV	S	(CH <sub>2</sub> ) <sub>3</sub> SO <sub>3</sub> <sup>-</sup>	2	C <sub>4</sub> H <sub>9</sub>	S	1
XVI	H <sub>3</sub> C—C—CH <sub>3</sub>	(CH <sub>2</sub> ) <sub>3</sub> SO <sub>3</sub> <sup>-</sup>	2	C <sub>4</sub> H <sub>9</sub>	O	2

dye which seemed to have a more sensitive fluorescence response. Table 4 also lists several other analogues of dye I, indicating that the negative charge was important (X–XIII), that the benzoxazole was better than the benzothiazole (XV) and that the thiobarbituric acid was better than the barbituric acid (IX and XVI). In addition to the diethyl substitution at  $R_2$  we also tried dipentyl (137) and dihexyl (138) which gave signals similar to that of dye I, as well as dimethyl (141), and dioctyl (140) which gave smaller signals than dye I. The signal-to-noise ratios that were obtained with the remaining dyes we tried on giant axons are given in the Appendix and further correlations between molecular structure and signal size can be determined from these results. It seems clear that signal size is relatively sensitive to small changes in dye structure.

### *Other Excitable Membranes*

Eighteen of the dyes used in experiments on squid axons were also tried on walking leg nerves from lobster. In all cases the changes in fluorescence during the compound action potential in the lobster nerve were in the same direction as the changes found during depolarizing steps in squid axon. In general, dyes which gave large changes in squid axons also gave large changes in lobster nerve. In addition, experiments with dye I on sensory neurons in segmental ganglia of the leech, *Hirudo medicinalis*, resulted in a  $\Delta I/I_r$ -sweep similar to that reported here for squid axons (Salzberg, Davila & Cohen, 1973). Finally, in preliminary experiments carried out with Murdoch Ritchie, Roger Tsien, and Richard Keynes on garfish (*Lepisosteus osseus*) olfactory nerve and on rabbit vagus nerve, the signal-to-noise ratio of the fluorescence change of dye I was an order of magnitude larger than the change in optical retardation (Cohen, Hille, Keynes, Landowne & Rojas, 1971; von Muralt, 1971). These results suggest that fluorescent dyes could be used to monitor membrane potential in any excitable membrane.

### *Two Anomalous Fluorescence Changes*

The intensity changes found with two dyes, malachite green (A) (added to the outside) and anthroyl stearic acid (H) (added outside or inside) were found to depend upon the time integral of the current (but not conductance), just as the current-dependent scattering changes did (Cohen *et al.*, 1972*b*). The similarity to the scattering changes was surprising because there was considerable evidence (Conti & Tasaki, 1970; Tasaki, Watanabe & Hallett, 1972; Davila *et al.*, 1974) that the changes in axon fluorescence were not

contaminated by artifacts from light scattering. In particular, fluorescence measurements made before the dye was added showed either no change or only a very small change during a potential step. Thus, simple interference from light scattering should be negligible. In addition, when the secondary filter (filter 2) was removed, so that scattering should be measured, a scattering change was found, but, it was similar to the scattering change normally observed at  $90^\circ$  (Cohen *et al.*, 1972*b*), while the anomalous intensity change found with the secondary filter in place was similar to the scattering change normally observed at  $10^\circ$  (Cohen *et al.*, 1972*b*). Although scattering-like fluorescence changes could result from light scattering changes that alter the amount of emitted light that reaches the photodetector, it is not clear why such changes were found with anthroyl stearic acid and malachite green but with no other dyes.

### *Potential Dependence*

The result in Fig. 3 suggested that the size of the fluorescence changes with dye I might be linearly related to the change in membrane potential. To test this hypothesis, the fluorescence of dye I was measured during a sweep with four different potential steps, and the results from such an experiment did fall along a straight line (Fig. 4). In addition to dye I, a few other dyes were studied in the same way, and the fluorescence changes of most of them (Fig. 4, legend) were linearly related to potential. However, the fluorescence changes of several dyes (Fig. 5, legend) were like that of brilliant basic red B (18) shown in Fig. 5*A*; two straight lines meeting at the origin fit the experimental points better than a simple linear relationship. The difference in slope of the two lines was largest with brilliant basic red B, but, with all such dyes, depolarizing steps gave larger fluorescence changes than did hyperpolarizing steps of the same size. However, even in these examples the time courses of the fluorescence changes for both steps were similar. In no case was there any indication of a fluorescence change with the time course of the conductance increase. Yet a third kind of potential dependence was exhibited by only one dye, coriphosphine O (9). The size of the fluorescence changes, measured with incident light of 570 nm, are plotted as a function of potential in Fig. 5*B*. The experimental points fell near the curve representing potential squared, with an origin 40 mV more depolarized than the resting potential. While all of the potential dependent retardation and light scattering changes were also related to the potential squared (Cohen *et al.*, 1971; Cohen *et al.*, 1972*a*), the change in coriphosphine O fluorescence is thus far the only optical effect symmetrical about a point near zero membrane potential.

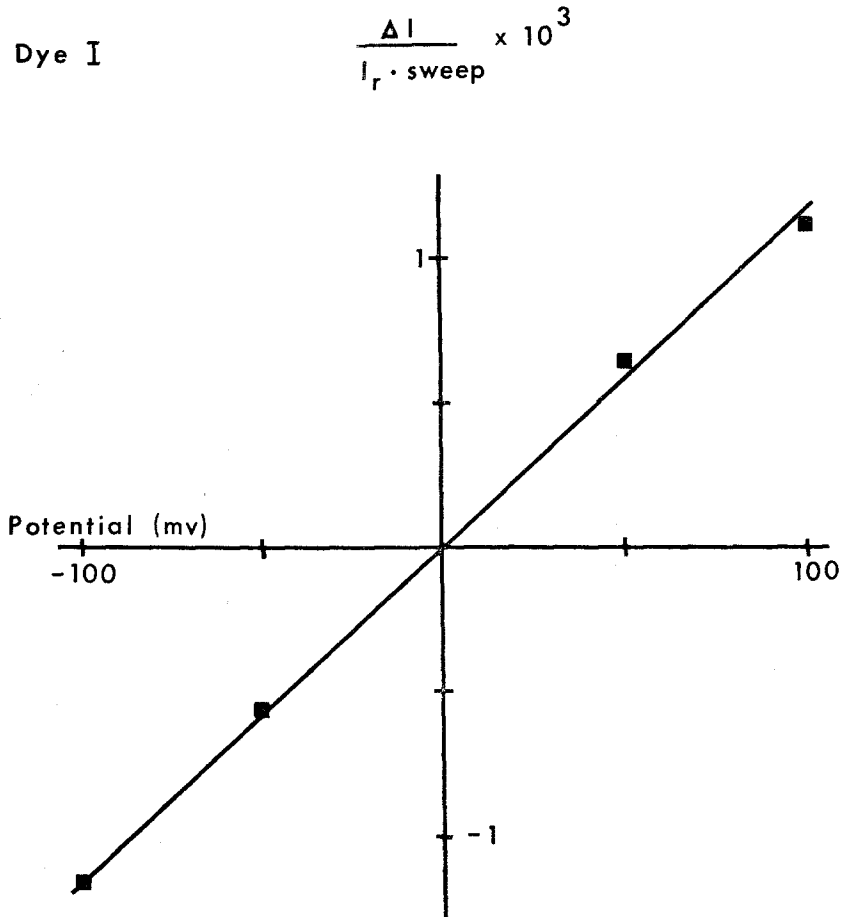


Fig. 4. Change in dye I fluorescence versus change in membrane potential. The fluorescence of dye I was related linearly to potential. The resting potential is zero mV on the abscissa. Other dyes whose fluorescence changes were linearly related to potential were: acridine orange (1), phosphine GN (7), rhodamine B (30), astrazone blue BG (21), cresyl violet acetate (23), astrazone red (222), quinoline blue (111), auramine O (255), intrawite CF (258), neutral violet (17), and 3,3'-dipentyl-oxacarbocyanine (64)

### *Time Courses*

Although the fluorescence of dye I shown in Figs. 2 and 3 seemed to change at the same time as the potential, when a much faster sweep speed was used, the fluorescence change was measurably slower than the change in potential. The top trace in Fig. 6 illustrates the results of such an experiment with dye I and also shows the time course of one of the slowest changes we have measured, that of dihexyl oxacarbocyanine (V) (middle trace). (Note that the time scale in the oxacarbocyanine experiment was about

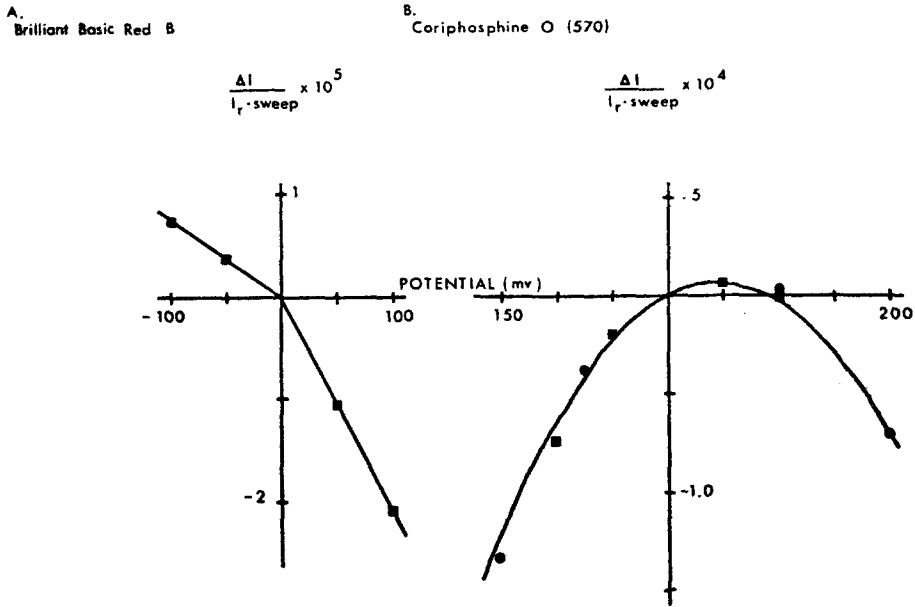


Fig. 5. Changes in axon fluorescence versus change in membrane potential for brilliant basic red B (18) and coriphosphine O (9). Two straight lines seemed to describe best the relationship between the fluorescence of brilliant basic red B and the potential, while the experimental points from two measurements with coriphosphine O fell near a curve having a square-law dependence on potential. The resting potential is zero mV on the abscissa. The excitation wavelengths were  $540 \pm 15$  nm and  $570 \pm 15$  nm, and the barrier filters (filter 2) were Schott OG 590 and RG 610, for brilliant basic red B and coriphosphine O, respectively. Some other dyes whose fluorescence changes were best fit by two straight lines were pyronin B (29), rhodamine S (28), brilliant cresyl blue (19), Nile blue A (24), quinaldine red (194), and dihexyloxacarbocyanine (V)

1,000 times slower than that for dye I.) At  $13^\circ\text{C}$  the fluorescence change of dye I occurred so rapidly that the averaged intensity change had to be corrected for the response time constant of the light-measuring system (in this experiment,  $35 \mu\text{sec}$ ) and the time constant of change in membrane potential (about  $10 \mu\text{sec}$ , Cohen *et al.*, 1971). When the measured time course was corrected for these effects, the fluorescence change for dye I was slower than the change in potential. The fluorescence change lagged behind the potential with a time course that could be approximated by a single exponential with a time constant of  $30 \mu\text{sec}$ . For the oxacarbocyanine fluorescence change, the sum of two exponentials was required, one with a time constant of  $3.1 \text{ msec}$  and the second with a time constant of  $130 \text{ msec}$ . The time constant(s) needed to approximate the time course of the fluorescence changes with other dyes ranged from  $30 \mu\text{sec}$  to  $100 \text{ msec}$ . (Because the responses of many dyes were slow compared to the 3-msec step used for



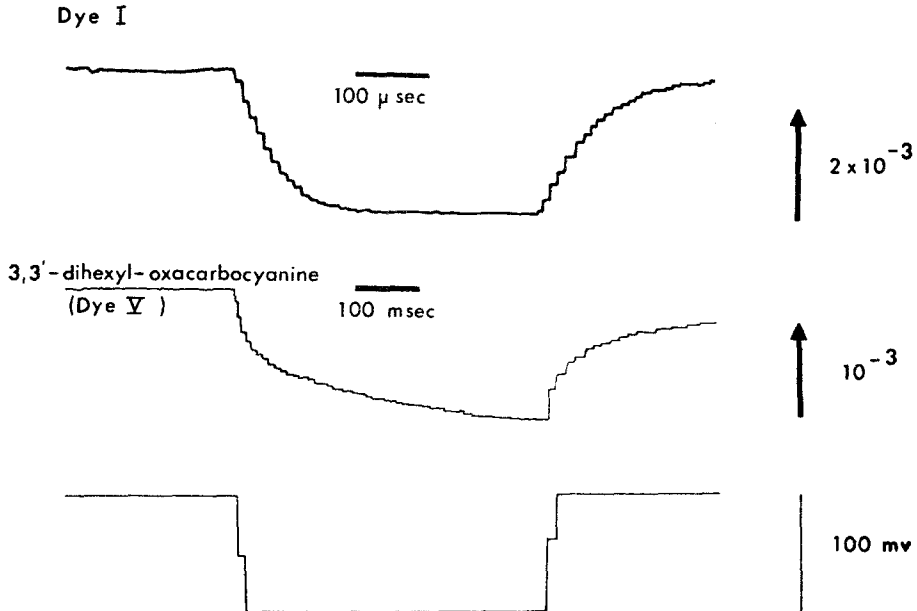


Fig. 6. Time course of the changes in dye I (top trace) and 3,3'-dihexyloxycarbocyanine (V) (middle trace) fluorescence resulting from a 100-mV hyperpolarizing step (bottom trace). The dye I fluorescence change, measured with a relatively fast sweep, was more than 1,000 times faster than the slow component of the dye VI change, measured with a slower sweep. The inward current densities at the end of the step were less than  $0.1 \text{ mA/cm}^2$ . The excitation wavelengths were  $570 \pm 15 \text{ nm}$  and  $480 \pm 15 \text{ nm}$  and the barrier filters (filter 2) were Schott RG 610 and OG 515 for dyes I and V, respectively. For the experiment with dye I the response time constant of the light measuring system was  $35 \mu\text{sec}$ ; 260 sweeps were averaged; for dye V, the response time constant was  $580 \mu\text{sec}$ ; and 8 sweeps were averaged. Temperature  $12^\circ\text{C}$

evaluating signal-to-noise ratios, the choice of a different step duration would lead to a different ordering of dyes in terms of signal size.) The long sweeps necessary to measure longer time constants were infrequently used, so there may be fluorescence changes of other dyes that are slower. In two experiments an attempt was made to measure the time course of the fluorescence change of dye I at a higher temperature ( $26^\circ\text{C}$ ), but the measured intensity change was fast compared to the experimental corrections, and we could only conclude that  $10 \mu\text{sec}$  was an upper limit to the time-constant at  $26^\circ\text{C}$ .

#### *Effect of Dye Concentration*

Incubation with several concentrations of dye in the range of 10 to  $1,000 \mu\text{M}$  were tried in an effort to find the concentration which resulted in the largest signal. With most dyes, one concentration within that range was

## Capri Blue (Dye VII)

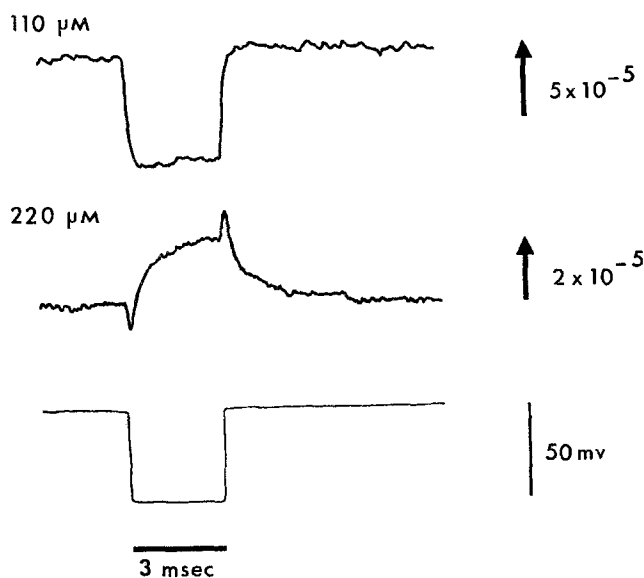


Fig. 7. Capri blue (dye VII) fluorescence changes after bathing in two different concentrations of the dye. With Capri blue, small changes in dye concentration led to large changes in the fluorescence signals. The axon was first incubated for 10 min in a 110  $\mu\text{M}$  solution of Capri blue in sea water. The dye solution was then replaced with sea water and the first measurement (top trace) was made. Twenty minutes later, the axon was incubated for 10 min in 220  $\mu\text{M}$  Capri blue. Following replacement of the dye solution by sea water, the second measurement was made. The hyperpolarizing potential step is shown in the bottom trace. The inward current density at the end of the step was less than 0.1  $\text{mA}/\text{cm}^2$ . Excitation wavelength was  $600 \pm 15 \text{ nm}$  and filter 2 was a Schott RG 645. The response time constant of the light measuring system was 180  $\mu\text{sec}$ ; 250 sweeps were averaged for the top trace, 1,000 sweeps were averaged for the middle trace. Temperature 11  $^{\circ}\text{C}$

optimal, and incubation at lower or higher concentrations resulted in qualitatively similar, but smaller, signal-to-noise ratios. However, with two oxazines, Capri blue (VII) and Nile blue A (24), relatively small increases in dye concentration in the incubation solution led to the appearance of a second fluorescence change. In the range 10 to 110  $\mu\text{M}$ , increasing the Capri blue concentration in the incubating solution led to larger signals, but, as Fig. 7 indicates, a further increase of the Capri blue concentration to 220  $\mu\text{M}$  led to a fluorescence change that seemed to be the sum of two components, the original fast decrease together with an increase that was slightly larger and slower in time course. Further increases in dye concentration led to a fluorescence change where the slow increase completely obscured the initial decrease. When the experiment was done using a high concentration ini-

tially, a result similar to the second trace in Fig. 7 was obtained, indicating that the effect shown in Fig. 7 did not result from a change in membrane properties as the axon aged (*see below*).

#### *Dye Added to the Inside of the Axon Membrane*

Because a dye which might serve as an optical indicator of membrane potential would be most useful if it could be added to the outside of the cell, most of our experiments were carried out with externally added dyes. However, a few dyes were also added to the inside of the membrane by microinjection into the axoplasm. The fluorescence changes of most dyes added internally were the same as the changes for the dyes added externally. (ANS was an exception; *see Davila et al.*, 1974.) Thus, hyperpolarizing steps led to an increase in pyronin B (29) fluorescence when the dye was added either externally or internally; both changes satisfied the criteria for potential dependence; and, as the axon deteriorated the fluorescence change of the internally added dye was altered in the same manner as the fluorescence change of externally added dye (*see below*). This qualitative similarity was also found with neutral red (13), neutral violet (17), acridine orange (1), auramine O (255) and rhodamine B (30), although the signal-to-noise ratios obtained for internally added dyes were always smaller. Three of these dyes, pyronin B, rhodamine B, and acridine orange, had previously been studied by Tasaki and collaborators (Tasaki *et al.*, 1969; Conti & Tasaki, 1970; Tasaki *et al.*, 1972). Our results were qualitatively similar to theirs, except that the pyronin B fluorescence change we found was similar to that shown in Fig. 2 of Conti and Tasaki (1970) and not similar to the result shown in Fig. 2 of Tasaki *et al.* (1972). When rhodamine B, pyronin B, neutral red and acridine orange were added externally, the extruded axoplasm was found to be stained at the end of the experiment. Thus, the similarity of the fluorescence changes for dyes added internally and externally might simply result from the accessibility of a binding site from either side of the membrane.

As part of the search for fluorescent probes of membrane conductance, two other dyes were specifically tested by addition to the inside of the membrane. We had hoped that anthroyl-TEA (*see Materials and Methods*) would behave like TEA itself and block the outward potassium currents (Armstrong & Binstock, 1965). But, as might have been predicted from its structure, the anthroyl-TEA functioned like a local anesthetic and preferentially blocked the increase in sodium conductance. The fluorescence signals that we measured in axons whose conductance changes had been partially blocked were symmetrical for hyperpolarizing and depolarizing steps and therefore provided no information about membrane conductance.

Caswell and Hutchison (1971) found that the fluorescence of membrane-bound chlorotetracycline (254) was greatly increased in the presence of calcium ions. Accordingly, we anticipated that the dye might be used as an indicator of calcium influx (Hodgkin & Keynes, 1957; Baker, Hodgkin & Ridgeway, 1971). However, both chlorotetracycline and tetracycline (253) blocked the membrane conductance increases at internal concentrations of about 50  $\mu\text{M}$ , and, as reported previously (Cohen *et al.*, 1971; Hallett, Schneider & Carbone, 1972), those fluorescence changes that could be measured were again symmetrical for hyperpolarizing and depolarizing steps. Thus, the tetracyclines also failed to provide information about structural events related to excitation.

#### *Wavelength Dependence*

The wavelength dependence of the fluorescence change was measured with a series of incident light filters of 30 nm width at half maximum and

peak transmittances 30 nm apart (from 450 to 690 nm). Usually the fluorescence change was largest with one of these filters, and excitation wavelengths of 30 and 60 nm on either side of the maximum led to smaller signals. For the dyes in Table 3 the wavelength for maximum signal is given in column 3.

However, with two dyes (71, 154) a more complex dependence on the wavelength of the incident light was found. With these dyes, the sign of the fluorescence signal depended on the wavelength of the incident light. A thiazoline-merocyanine (154) gave a decrease in fluorescence intensity during depolarizations when the incident wavelength was 540 or 570 nm but an increase with 630 and 660 nm. The time course and potential dependence at both wavelengths were similar, suggesting that the increase and decrease might be explained by the same process, e.g., a structural change in the membrane that led to a shift in the absorption maximum of the dye. At one wavelength this would result in an increase in fluorescence; at another wavelength a decrease would result.

#### *Changes in the Fluorescence Signal as the Axon Aged*

The results above were obtained when the axons were in good condition; i.e., the peak inward current during a 50-mV depolarizing step was more than 1.3 mA/cm<sup>2</sup>. With many dyes, the fluorescence change altered in character as the axon's condition deteriorated. The simplest alteration was a change in the size of the signal. When the axons were in poor condition, the signal-to-noise ratio obtained with dihexyloxacarboxyanine (V) increased by a factor of 6 over the value reported in Table 3. The increase in size seemed to be directly related to the condition of the axon; in axons which remained in good condition for hours the fluorescence change remained relatively small for hours. These "dead-axon dyes" were a source of annoyance because many experiments were wasted in an effort to obtain large changes in a healthy axon.

The fluorescence of several xanthene dyes increased during hyperpolarizing steps when the axon was in good condition. However, with each of these xanthenes, as the axon deteriorated, a second signal was observed which was in the opposite direction. Fig. 8 illustrates such a result with the dye pyronin B (29). In this case, the second signal had a time course that was much slower than that of the original signal, so that when the axon was beginning to run down, both signals could be observed. These changes in the fluorescence signals that occurred as the axon deteriorated suggest that rather widespread structural alterations may accompany the loss of excitability.

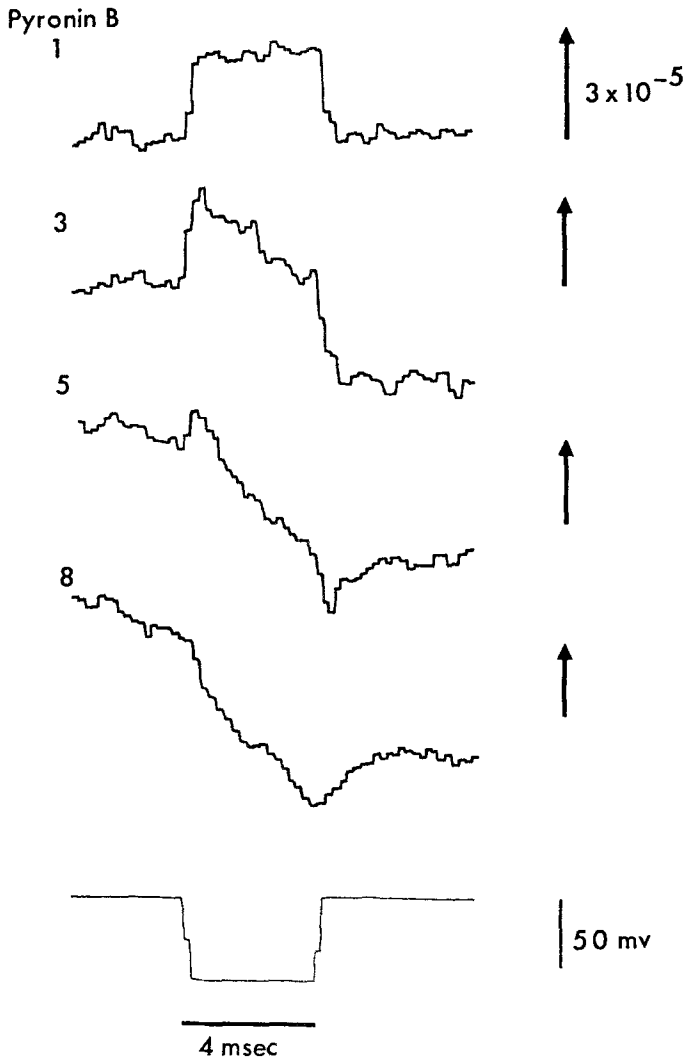


Fig. 8. Pyronin B (29) fluorescence changes in the first (top trace), third (second trace), fifth (third trace), and eighth (fourth trace) trial on the same axon. As the axon deteriorated a second component in the fluorescence appeared, and grew larger. The inward current density during the hyperpolarizing step (bottom trace) was less than  $0.1 \text{ mA/cm}^2$  for the first trace and was  $0.3 \text{ mA/cm}^2$  for the fourth trace. The peak inward current density during a 50-mV depolarizing step declined from  $2.2 \text{ mA/cm}^2$  at the time of the first trace to  $0.1 \text{ mA/cm}^2$  at the time of the eighth trial. Each arrow represents a  $\Delta I/I_r$ -sweep of  $3 \times 10^{-5}$ . The axon was first incubated in  $30 \text{ } \mu\text{M}$  pyronin B sea water, and the experiments were carried out in the presence of  $5 \text{ } \mu\text{M}$  pyronin B. The excitation wavelength was  $510 \pm 15 \text{ nm}$  and filter 2 was a Schott OG 550. The response time constant of the light measuring system was  $240 \text{ } \mu\text{sec}$  and 2,000 sweeps were averaged for each trace. Temperature  $10^\circ \text{C}$

### *Photodynamic Damage*

An important factor limiting the use of fluorescence as a monitor of membrane potential is the photodynamic damage to the membrane (Arvanitaki & Chalazonitis, 1961; Pooler, 1972) that occurs with some dyes at high incident light intensities in the presence of oxygen. While most experiments were carried out in a nitrogenated sea water and no photodynamic damage was observed, a few experiments were designed to measure the photodynamic damage by monitoring the light dependent reduction of inward current in sea water equilibrated with air. With dye I the inward current was reduced by 50% in about 10 sec. The same rate was found with the indolenine derivative (IX), but with several other dyes including (122), an analogue of (IV), the reduction to 50% took about 100 sec. Capri blue (VII) and Nile blue A (24) also seemed to have less photodynamic damage. The amount of photodynamic damage was thus also dependent upon dye structure, and it should therefore be possible to design dyes which minimize this effect.

### **Discussion**

We attempted to measure changes in axon fluorescence using more than 300 dyes, and we succeeded with about 180 of them. In every case but two (malachite green and anthroyl stearic acid), where the signal-to-noise ratio was large enough to permit a judgment, the fluorescence changes had the same time course during hyperpolarizing and depolarizing potential steps. Since only the depolarizing steps led to large ionic currents and increased membrane conductance, the similarity in time course indicated that the fluorescence changes were related to membrane potential.

The fluorescence changes of several dyes were larger during depolarizing steps than during hyperpolarizing steps of the same size (Fig. 5A). While it might be supposed that this would constitute evidence for a conductance dependence of some sort, there are several potential-dependent mechanisms that could give such a result. For example, an electric field-induced movement of a membrane-bound fluorescent molecule might be greater toward the center of the membrane than the corresponding movement toward the outside. One could argue, of course, that any of the faster fluorescence changes are indicating some structural event in the process that converts membrane depolarization into increased membrane conductance and that these structural events are symmetrical about the resting potential even though the conductance increases that they ultimately lead to are not. Such hypotheses could be so flexible as to obviate any attempt to disprove them. We

feel that there is no evidence that would directly link any of the fluorescence changes yet measured to the increases in membrane conductance that underlie the action potential.

Since only a few tetrodotoxin molecules bind to each square micron of axon membrane (Moore, Narahashi & Shaw, 1967; Colquhoun, Henderson & Ritchie, 1972), it seems possible that only a small fraction of the membrane area is directly involved with the conductance changes. Perhaps, then, it is not surprising that none of the fluorescence changes is related to membrane conductance. Most of the dyes we tried did not affect the conductance mechanisms and we presume that their binding depends upon nonspecific physical and chemical affinities (Beyer, Craig & Gibbons, 1973). If that were the case, most of the dye molecules bind in areas not directly involved with the conductance changes. Then, the changes in the potential gradients and any associated structural alterations would be expected to give rise to fluorescence changes that would obscure any change that resulted from the few dye molecules bound to sites where the conductance increases are regulated. Consequently, we feel that the synthesis of fluorescent analogues of molecules such as tetrodotoxin, with great site specificity, is the most promising approach if fluorescence changes related to membrane conductance are to be found.

While the search for fluorescence changes related to membrane conductance was unsuccessful, we did find several fluorescence signals that were relatively large. Gary Strichartz suggested that we try merocyanine dyes, and Eastman Research Laboratories supplied us with samples of several such molecules. The fluorescence change of one of these, dye I, was one of the largest that we measured in healthy axons. The top trace in Fig. 9, a photograph of a single oscilloscope sweep, shows the fluorescence increase of this dye during an action potential (bottom trace). This fluorescence change is obviously large enough to function as an optical indicator of the occurrence of action potentials in a giant axon. The large signal-to-noise ratio shown in Fig. 9 was achieved without signal averaging by limiting the bandwidth of the light-measuring apparatus in comparison with the bandwidth used for Fig. 2. Several of the dyes in Table 3 might serve as optical indicators of membrane potential in systems where more membrane area can be monitored, and preliminary reports of such experiments on red blood cells, mitochondria, synaptosomes, and muscle have already appeared (Chance, 1973; Goldring & Blaustein, 1973; Bezanilla & Horowicz, 1974; Hoffman & Laris, 1974; Landowne, 1974). Hoffman and Laris found that an oxacarboxyanine (V) was more useful than dye I in their experiments. While this may result from differences in membrane properties of squid

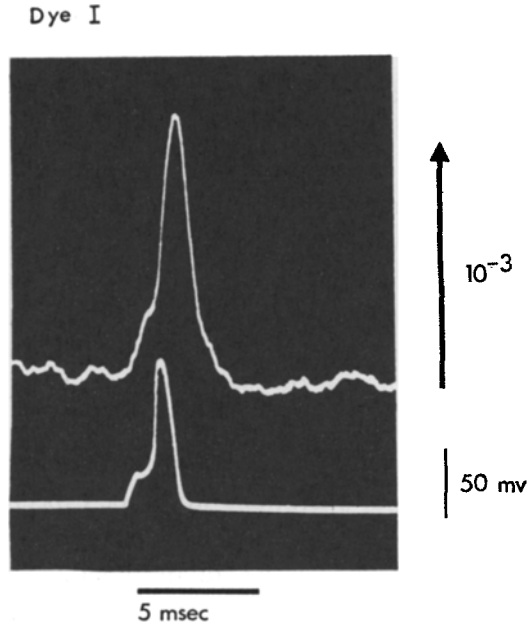


Fig. 9. Dye I fluorescence change (top trace) during an action potential (bottom trace). A single oscilloscope sweep was photographed; no signal averaging was required. The rising phase of the electrically recorded action potential was retouched. The excitation wavelength was  $570 \pm 15$  nm and filter 2 was a Schott RG 610. The time constant of the light measuring system was 600  $\mu$ sec

axon and human red blood cells, experiments using longer potential steps (Fig. 6) suggest that the differences in the time scale of the experiments (milliseconds in axons, seconds in red blood cells) is an important factor.

Malley, Feher and Mauzerall (1968) and Emrich, Junge and Witt (1969) have suggested that electrochromic shifts in the absorption of membrane-bound molecules could be used to monitor membrane potential. Thus far, in the chloroplast membrane studied by Emrich *et al.* (1969), there have been no independent measurements of membrane potential to confirm this suggestion. Also, it seems likely that the fluorescence changes reported here will be more convenient for monitoring membrane potential because of their larger signal-to-noise ratios.

The fluorescence of dye I increased by about 0.2% during an action potential (Figs. 2 and 9). Since it is unlikely that all of the dye was bound to the axon membrane, the change in membrane fluorescence was probably larger than 0.2%. If we assume that the dye did not cross the axon or Schwann cell membranes, and that it was bound only to membrane, then the change in axon membrane fluorescence would be about 1% because



the axon membrane comprises about 20% of the external membrane in a giant axon (Camejo, Villegas, Barnola & Villegas, 1969; Villegas, 1969). With different assumptions, the change in membrane fluorescence would be larger than 1%, but it seems unlikely to be smaller.

Optical methods of measuring potential could be used to follow activity in central nervous systems (Salzberg *et al.*, 1973). An apparatus with a large number of photodiodes, arranged so that each detector received the light from an individual cell body, could simultaneously monitor the activity of, perhaps, 100 neurons in an invertebrate ganglion. Such cell bodies are, however, considerably smaller than the 5-mm length of giant axon used in our experiments. Assuming that geometry, incident-light intensity, dye-binding, and fluorescence sensitivity are unchanged, the signal-to-noise ratio will be smaller for a smaller cell; with dye I, the signal-to-noise ratio during a 100-mV action potential in a 150  $\mu\text{m}$  spherical cell would be reduced to 2:1. [The signal-to-noise ratio of 5:1 in a 50- $\mu\text{m}$  leech neuron (Salzberg *et al.*, 1973) was obtained by increasing the incident intensity.] Clearly, even larger fluorescence changes than those reported in Tables 3 and 4 would be very useful.

The search for better probes would be facilitated if we knew why the fluorescence signals of some molecules were large and if we understood the physical mechanism(s) giving rise to the fluorescence changes. We have tried two approaches to this problem: a study of the variation in signal size with analogues of particular dyes, and a comparison of spectral properties of the fluorescent molecules with the size of the changes.

The results in Table 4 show that the charge on the dye is an important determinant of signal size since positively charged (XIII) and neutral (XII) analogues gave much smaller signals than did the negatively charged dye (XI). But dyes I and IV in Table 3 show that negatively and positively charged dyes (of different types) can give rise to relatively large fluorescence changes of the same sign, and comparison of VII with 30 shows that dyes with the same charge can give rise to fluorescence changes of opposite sign. Thus, it is clear that while charge is important, it is not a unique determinant of signal magnitude or direction. The comparison of the dimethyl (141) and diethyl (XI) analogues with dye I shows that the hydrophobicity of the dye is also an important determinant of signal size. In this series, the more hydrophobic the dye the larger the signal. But just the opposite effect was found for the ethyl through decyl quinaldine reds (194 to 197); the more hydrophobic the dye the smaller the signal. While the hydrophobicity of the dye is also important, it is not a uniquely determining factor.

Table 5. Spectral properties of three merocyanines: I, 158 and 151

Dye	Solvent	$\lambda_{\text{MAX}}^{\text{ABS}}$	$\epsilon \times 10^2$	$\lambda_{\text{MAX}}^{\text{FL}}$	$I_{\text{FL}}^a$	$S/N$ in axon experiments
I	water	500	58	572	0.05	5.0
	ethanol	558	175	580	1.05	
158	water	622	55	661	0.18	0.08
	ethanol	641	141	670	0.59	
151	water	535	39	585	0.06	<0.01
	ethanol	572	188	594	1.25	

<sup>a</sup>  $I_{\text{FL}}$  gives the emission intensity per mole of dye measured in a narrow bandwidth at the emission maximum when the dye was excited at its absorption maximum. These values were corrected for variations of instrument sensitivity with wavelength and are normalized to  $I_{\text{FL}} = 1.0$  for 5-[(3-ethyl-2(3H)-benzoxazolyliidene)-2-butenylidene]-1,3-diethyl-2-thiobarbituric acid (XII) used as a standard. Some merocyanines tend to dimerize in water (*see* West & Pearce, 1965). The values given in the table are from dilute solutions where the monomer predominates.

Another property of dye molecules which should be related to signal size is their absorption and emission spectra. It was difficult to choose solvents that would model different regions of the axon membrane because the spectral properties of many dyes are sensitive to specific solvent interactions rather than general solvent properties; and it is not possible, in general, to find solvents which differ in only one physical property. Since spectra measured in glycerol at various temperatures suggested that the fluorescence of some cyanine dyes was viscosity dependent, we compared the spectral properties of the dyes in water and ethanol. The viscosities of water and ethanol differ by a relatively small amount (20 % at 20 °C), but ethanol has a dielectric constant only one-third that of water, so that this comparison should mainly reflect differences in dielectric constants. Table 5 lists the absorption and emission peaks, the absorption coefficients, and the relative fluorescence intensities for three merocyanines, I, 158 and 151. These molecules were chosen for spectral studies because they were examples of substances of rather similar structure which gave signals that were very different in size. The signal with dye I was 60 times larger than that of 158 and at least 500 times larger than that of 151. As Table 5 indicates, for the three merocyanines, the absorption coefficient, emission intensity, wavelength maxima and their shifts in going from water to ethanol were quite similar. Therefore, there was no clue from these spectroscopic measurements that could help to explain the differences in signals from the three dyes; all three were

sensitive to solvent polarity. On the other hand, the solubilities of the three merocyanines were quite different. Dye I was about equally soluble in decane and water, while 158 was much more soluble in decane than in water, and 151 was nearly insoluble in both solvents.

It seems difficult at this stage to determine what can be learned about axon structure from any of the fluorescence changes. For example, the fluorescence of dye I depends on solvent polarity, viscosity, temperature and its specific chemical neighbors (A. S. Waggoner, *unpublished results*). In addition, it is a member of a class of dyes where the electric field has direct effects on absorption (electrochromism) and possibly on emission (Platt, 1962; Bücher, Wiegand, Snively, Beck & Kuhn, 1969). Although a direct effect of the electric field on absorption seems unlikely to explain the changes in axon fluorescence because the changes were slower than and much larger than reported electrochromic effects, we have no evidence about which of the other environmental variables are changing to give rise to the fluorescence signals. In addition, we do not know why the environment of the dye is altered. It could be that the structure of the membrane is changing. On the other hand, the changing electric field might lead to movement or rotation of the dye or to changes in the amount of dye bound to the membrane. The linear dependence of the dye I fluorescence on membrane potential does argue against dipole rotation alone, but it seems impossible to decide from our experiments which of the other mechanisms might be important. In experiments on red blood cells, Sims, Wang, Waggoner and Hoffman (1974) measured potential-dependent changes in fluorescence using dye 72 and showed that the changes in fluorescence occurred because of changes in the amount of dye bound to the membrane. In nerve membranes changes in the binding of neutral red and direct turquoise occur as a result of trains of action potentials (Nasonov, 1962; Levin, Rozenthal and Komissarchik, 1968), so potential-dependent changes in dye binding may be an important factor in explaining the fluorescence changes.

In red blood cells Sims *et al.* (1974) found that the fluorescence changes of dye 72 were accompanied by changes in the absorption spectrum of the dye, suggesting the possibility that the signals described in this paper as changes in fluorescence may, in fact, result purely from changes in dye-absorption spectra.

We are indebted to the director and staff of the Marine Biological Laboratory for their assistance and to the Eastman Research Laboratories for providing several merocyanine dyes. Supported by U.S. Public Health Service grants NS 08437, NS 10489, and NB 08304 from the National Institute of Neurological Diseases and Stroke.

## Appendix

### *Fluorescence Changes of Additional Dyes Applied Externally to Squid Giant Axons<sup>1</sup>*

The signal-to-noise ratio of the change in fluorescence for a single 50-mV hyperpolarizing voltage-clamp step and the source of the dye according to the list in Table 1 are given in parentheses. The designation "n.c." indicates that no fluorescence change was observed (signal-to-noise ratio < 0.02). The trinuclear heterocyclic, azo, and triphenylmethane dyes are listed according to the classification in the third edition of the Colour Index (1971); the classification and nomenclature of most of the remaining dyes conform to that of Hamer (1964). Within groups, the dyes are listed so that similar structures are near one another. Structural formulae are available from the authors. Dyes from Nippon Kankoh-Shikiso Kenkyusho, Ltd., Okayama, Japan (NK) are designated by the catalogue number in the company's organic chemical list (1969). The fluorescence changes of several dyes were very different in size or different in sign from axon to axon and were not included below. These were (with source in parentheses): acridine red (D), fast acid violet 10B (C), Janus black (E), fast blue B salt (A), methoxyacridine (L), azocarmine G (D), methylene violet (A), safranin O (D, J), astra violet (A), astra phloxine (A) and rhodamine 6G (D). The signal-to-noise ratios in a single sweep were less than 0.2 with these dyes.

#### Trinuclear Heterocyclic Dyes

*Acridines.* 1. acridine orange (0.3, K); 2. acridine yellow (n.c., D); 3. brilliant phosphine (0.02, A); 4. acriflavine (0.02, D); 5. atebirin (0.1, E); 6. phosphine 3R (0.07, A); 7. phosphine GN (0.06, D); 8. benzoflavine (n.c., C); 9. coriphosphine O (0.02, 0.02, E, F); 10. 9(10H) acridine (n.c., L); 11. dodecylaminoacridine (n.c., X); 12. octadecylaminoacridine (n.c., X).

*Amino azines.* 13. neutral red (0.3, B, C); 14. neutral red acetamide (n.c., H); 15. neutral red butylamide (0.02, H); 16. neutral red octylamide (0.02, H); 17. neutral violet (0.1, I); 18. brilliant basic red B (0.09, U, W).

*Oxazines.* 19. brilliant cresyl blue (0.6, D, F); 20. cresyl fast violet acetate (0.05, E); 21. astrazone blue BG (0.2, O); 22. Zapon fast blue 3G (0.7, W); 23. cresyl violet acetate (0.2, D); 24. Nile blue A (0.8, D); 25. Darrow red (n.c., C); 26. Nile pink (0.7, D).

*Xanthenes.* 27. pyronin Y (0.3, M); 28. rhodamine S (0.3, F); 29. pyronin B (0.08, D); 30. rhodamine B (0.5, D); 31. rhodamine 3B (1.6, N); 32. sulphorhodamine (n.c., A); 33. eosin Y (0.02, B); 34. eosin B (n.c., B); 35. fluorescein dibutyrate (n.c., M); 36. dichlorofluorescein (n.c., M).

*Thiazines.* 37. thionin (n.c., A); 38. azure B (n.c., D); 39. methylene blue (n.c., D); 40. toluidine blue O (0.02, B).

1 An additional 16 dyes were tried only on lobster nerve. Fluorescence changes were found with phenosafranin (A), procion yellow M4R (V), euchrysin 2GNX (E), proflavine (D), primuline (A), aurophosphine (K), thiazol yellow (A), Meldola's blue (E) and ponceau 2R (A); but, with each of these dyes, the signal-to-noise ratio was smaller than that found with acridine orange (1). No fluorescence changes could be measured in lobster nerve with gallocyanin (A), resorcin blue (A), amethyst violet (F), Janus green B (E), thioflavine T (A), ethyl (diquinoline) red (M), or Congo red (D).

## Azo Dyes

41. azorubin S (n.c., A); 42. orange IV (n.c., D); 43. chrysoidin Y-special (n.c., D); 44. tartrazine O (n.c., A); 45. Bismarck brown (n.c., A); 46. thiazine red R (n.c., A); 47. Janus red (n.c., E); 48. yellow AB (n.c., F); 49. Maxilon blue RL (n.c., E); 50. solochrome violet RS (0.02, A); 51. astrazone red F3BL (n.c., O).

## Triphenylmethane Dyes

52. acid violet 6B (0.05, A); 53. aniline blue (n.c., B); 54. bromthymol blue (n.c., B); 55. brilliant dianile green (n.c., A); 56. gentian violet (0.2, A); 57. methyl blue (n.c., A).

## Cyanine Dyes (Including Hemicyanines)

58. dicyanine A (n.c., G); 59. Basic Yellow 13 (n.c., P); 60. 3,3'-dimethyl-oxacyanine iodide (n.c., NK 503); 61. 3,3'-diethyl-oxacarboxyanine iodide (0.4, H); 62. 3,3'-dipropyl-oxacarboxyanine iodide (0.6, H); 63. 3,3'-dibutyl-oxacarboxyanine iodide (0.6, H); 64. 3,3'-dipentyl-oxacarboxyanine iodide (0.3, H); 65. 3,3'-didecyl-oxacarboxyanine iodide (0.06, H); 66. 3,3'-dioctadecyl-oxacarboxyanine iodide (n.c., H); 67. 3,3'-diethyl-oxadicarboxyanine iodide (0.15, M); 68. 3,3'-diethyl-thiacarboxyanine iodide (0.4, H); 69. 3,3'-dipropyl-thiacarboxyanine iodide (0.08, H); 70. 3,3'-diethyl-thiacarboxyanine iodide (0.15, H); 71. 3,3'-diethyl-thiadicarboxyanine iodide (0.2, H); 72. 3,3'-dipropyl-thiadicarboxyanine iodide (0.03, H); 73. 3,3'-diethyl-thiadicarboxyanine iodide (0.2, H); 74. 3,3'-ditetradecyl-thiadicarboxyanine iodide (n.c., H); 75. 3,3'-diethyl-thiatricboxyanine iodide (0.1, H); 76. anhydro-3,3'-di- $\gamma$ -sulfo-3-propyl-thiacarboxyanine hydroxide (0.08, H); 77. anhydro-3- $\gamma$ -sulfo-3-propyl-3'-decyl-thiadicarboxyanine hydroxide (0.04, H); 78. anhydro-3,3'-di- $\gamma$ -sulfo-3-propyl-thiadicarboxyanine hydroxide (n.c., H); 79. 3,3'-diethyl-6,6'-di-methoxy-thiacarboxyanine iodide (n.c., NK 535); 80. 3,3'-diethyl-4,5,4',5'-dibenzothiacarboxyanine iodide (n.c., NK 382); 81. 3,3'-diethyl-*meso*-chlorothiadicarboxyanine iodide (n.c., NK 74); 82. 3,3'-bis-( $\beta$ -hydroxyethyl)-5,5'-dimethyl-*meso*-methyl-thiacarboxyanine bromide (n.c., NK 1410); 83. 3,3'-diethyl-*meso*-phenylthiacarboxyanine iodide (1.8, NK 1507); 84. 3,3'-diethyl-*meso*-methylthiothiacarboxyanine iodide (0.3, NK 1071); 85. 3,3'-diethyl-*meso*-*m*-nitrophenylthiacarboxyanine iodide (n.c., NK 1455); 86. 3,3'-diethyl-*meso*-(*p*-dimethylaminostyryl)-thiacarboxyanine iodide (n.c., NK 94); 87. 3,3'-diethyl-*meso*-( $\beta$ -2-furylvinyl)-thiacarboxyanine iodide (n.c., NK 95); 88. 3,3'-diethyl-selenacarboxyanine iodide (0.4, NK 616); 89. 2-[6-(1-piperidyl)-1,3,5-hexatrienyl]-benzothiazole ethiodide (0.4, NK 439); 90. 3,3'-diethyl-thiazolinocarboxyanine iodide (n.c., NK 1045); 91. 3,3'-diethyl-thiazolinodicarboxyanine iodide (0.2, H); 92. 3,3',4,4'-tetramethyl-thiazolocarboxyanine iodide (n.c., NK 15); 93. 3,3',4,4'-tetramethyl-5,5'-dicarboxylthiazolocarboxyanine iodide (0.05, NK 1510); 94. 3,3'-diethyl-4,4'-dimethyl-5,5'-dicarboxy-*meso*-ethylthiazolocarboxyanine iodide (0.5, NK 1458); 95. 3-ethyl-2-[5-(3-ethyl-2-benzothiazoinylidene)-1,3-pentadienyl] benzothiazolium iodide (0.07, M); 96. 3,3'-diethyl-4,4'-dimethyl-5,5'-dicarboxy-*meso*-(4-methyl-5-carboxy-2-thiazolyl ethiodide) thiazolodicarboxyanine iodide (1.0, NK 35); 97. 3,3'-diethyl-4,4'-dimethyl-*meso*-(4-methyl-2-thiazolyl ethiodide) thiazolodicarboxyanine iodide (n.c., NK 13); 98. 5,5'-bis-(3-ethyl-4-methyl-2(3H)-thiazolylidene)-4,4'-dioxo-3,3'-diethyl-thiazolinocyanine sulfonate (n.c., NK 1468); 99. 3,3',4,4'-tetramethyl-*meso*-(4-methyl-2-oxazolyl methiodide) oxazolodicarboxyanine iodide (n.c., NK 325); 100. 1-ethyl-2-[(1,4-dimethyl-2-phenyl-6-pyrimidinylidene)-methyl] quinolinium chloride (0.15, M); 101. 1,1'-diethyl-*meso*-[(1-ethyl-2(1H)-quinolylidene)-methyl]-2,2'-carbocyanine iodide (0.02, NK 222); 102. 1,1'-diethyl-4,4'-dicarboxyanine iodide (0.03, NK 1144); 103. 1'-ethyl-6'-ethoxy-1,3,3-trimethylindo-2'-carbocyanine iodide (0.07, NK 1131); 104. 1,1'-diethyl-*meso*-(acetoxy)-2,2'-tetracarboxyanine iodide (n.c., NK 1161); 105. 1,1'-diisopentyl-4,4'-

carbocyanine iodide (0.2, NK 45); 106. 2- $[\beta$ -(1-piperidyl)-vinyl]-quinoline ethiodide (n.c., NK 617); 107. 4- $[\beta$ -(1-piperidyl)-vinyl]-quinoline ethiodide (n.c., NK 645); 108. 1,1'-diethyl-4,4'-carbocyanine iodide (cryptocyanine) (0.1, M); 109. 1,1'-diethyl-2,2'-cyanine iodide (pseudoisocyanine) (0.02 M, H, Q); 110. 1,1'-diethyl-2,2'-carbocyanine iodide (pinacyanole) (0.01, C); 111. 1,1'-diisoamyl-4,4'-cyanine iodide (quinoline blue) (0.2, F); 112. 1,1'-diethyl-6,6'-bis-(dimethylamino)carbocyanine iodide (0.16, NK 537); 113. 1,1'-dimethyl-2,3,2',3'-dibenzo-*meso*-(9-acridinyl methiodide)-4,4'-dicarbocyanine iodide (n.c., NK 20); 114. 1,1'-diethyl-*meso*-(4-quinolyl ethiodide)-4,4'-dicarbocyanine iodide (n.c., NK 4); 115. 1,1'-diethyl-6,6'-dimethylamino-*meso*-(2-quinolyl ethiodide)-2,2'-dicarbocyanine iodide (n.c., NK 539); 116. 1,3,3,1',3',3'-hexamethyl-indocyanine iodide (n.c., NK 388); 117. 1,3,3,1',3',3'-hexamethyl-indocarbocyanine iodide (acronol ploxine FFS) (0.8, W); 118. 1,3,3,1',3',3'-hexamethyl-5,5'-diacetamido-indocarbocyanine iodide (Astra Violet) (0.2, A); 119. 1,1'-dipropyl-3,3,3',3'-tetramethyl-indocarbocyanine iodide (1.7, H); 120. 1,1'-dipentyl-3,3,3',3'-tetramethyl-indocarbocyanine iodide (1.3, H); 121. anhydro-1,1'-di- $\gamma$ -sulfofpropyl-3,3,3',3'-tetramethyl-indocarbocyanine hydroxide (pyridine salt) (n.c., NK 1639); 122. 1,3,3,1',3',3'-hexamethyl-indodicarbocyanine iodide (3.6, NK 529); 123. anhydro-1,1'-dicarboxymethyl-3,3,3',3'-tetramethyl-indodicarbocyanine hydroxide (n.c., NK 1679); 124. 1,3,3,1',3',3'-hexamethyl-indotricarbocyanine iodide (0.9, NK 125); 125. 1,1'-dicarboxymethyl-3,3,3',3'-tetramethyl-*meso*-chloroindodicarbocyanine iodide (0.2, NK 1680); 126. 1,3,3,1',3',3'-hexamethyl-*meso* (3,3-dimethyl-2(3H)-indolyl methiodide)-indodicarbocyanine iodide (1.4, NK 540); 127. 1,3,3,3'-tetramethyl-indoxacyanine iodide (n.c., NK 1684); 128. 1'-ethyl-1,3,3-trimethylindo-4'-carbocyanine iodide (0.5, NK 323); 129. 1'-heptyl-1,3,3-trimethylindo-2'-carbocyanine iodide (0.4, NK 303); 130. 3'-ethyl-6',7'-benzo-1,3,3-trimethyl-indoxacarbocyanine iodide (0.4, NK 1519); 131. astrazone orange G (0.07, O, D).

#### Merocyanine Dyes

132. 5-[(3,3-dimethyl-1- $\gamma$ -sodium-sulfofpropyl-2(3H)-indolylidene)-2-butenylidene]-1,3-dipropyl-2-thiobarbituric acid (3.0, H); 133. 5-[(3,3-dimethyl-1- $\gamma$ -sodium sulfofpropyl-2(3H)-indolylidene)-2-butenylidene]-1,3-dihexyl-2-thiobarbituric acid (5.0, H); 134. 5-[(3,3-dimethyl-1- $\beta$ -sodium-carboxyethyl-2(3H)-indolylidene)-2-butenylidene]-1,3-dibutyl-2-thiobarbituric acid (0.9, H); 135. 5-[(3,3-dimethyl-1-propyl-2(3H)-indolylidene)-2-butenylidene]-1,3-dibutyl-2-thiobarbituric acid (0.3, H); 136. 2-[(1,3,3-trimethyl-2(3H)-indolylidene)-ethylidene]-3(2H)-thianaphthenone (0.5, NK 1183); 137. 5-[(3- $\gamma$ -sodium-sulfofpropyl-2(3H)-benzoxazolylidene)-2-butenylidene]-1,3-dipentyl-2-thiobarbituric acid (4.9, H); 138. 5-[(3- $\gamma$ -sodium-sulfofpropyl-2(3H)-benzoxazolylidene)-2-butenylidene]-1,3-dihexyl-2-thiobarbituric acid (4.5, H); 139. 5-[(3- $\gamma$ -sodium-sulfofpropyl-2(3H)-benzoxazolylidene)-2-butenylidene]-1-ethyl-3-octyl-2-thiobarbituric acid (4.7, H); 140. 5-[(3- $\gamma$ -sodium-sulfofpropyl-2(3H)-benzoxazolylidene)-2-butenylidene]-1,3-dioctyl-2-thiobarbituric acid (0.7, H); 141. 5-[(3- $\gamma$ -sodium-sulfofpropyl-2(3H)-benzoxazolylidene)-2-butenylidene]-1,3-dimethyl-2-thiobarbituric acid (0.02, H); 142. 5-[(3- $\gamma$ -sodium-sulfofpropyl-2(3H)-benzoxazolylidene)-2-butenylidene]-1-ethyl-3-octadecyl-2-thiobarbituric acid (n.c., H); 143. 5-[(3- $\gamma$ -sodium-sulfofpropyl-2(3H)-benzoxazolylidene)-2-butenylidene]-1,3-dimethylbarbituric acid (n.c., H); 144. 5-[(3- $\gamma$ -sodium-sulfofpropyl-5-methoxy-2(3H)-benzoxazolylidene)-ethylidene]-1,3-diethyl-2-thiobarbituric acid (n.c., M); 145. 5-[(3- $\beta$ -carboxyethyl-2(3H)-benzoxazolylidene)-2,4-hexadienylidene]-1,3-di- $\beta$ -methoxyethyl-barbituric acid (n.c., M); 146. 5-[(3-ethyl-2(3H)-benzoxazolylidene)-ethylidene]-1-ethyl-3-( $\beta$ -dimethylaminoethyl hydrobromide)-barbituric acid (n.c., M); 147. 5-[(3- $\gamma$ -sodium-sulfofpropyl-2(3H)-benzothiazolylidene)-2,4-hexadienylidene]-1,3-diethyl-2-thiobarbituric acid (0.04, H); 148. 5-[(3-ethyl-2(3H)-benzothiazolylidene)-2-butenylidene]-1,3-diethyl-2-thiobarbituric acid (0.01, H); 149. 5-[(3- $\gamma$ -propyltrimethylammonium bromide-2(3H)-benzothiazolylidene)-

2-butenylidene]-1,3-dibutyl-2-thiobarbituric acid (0.01, H); 150. 5-[(3- $\gamma$ -sodium-sulfopropyl-2(3H)-benzothiazolylidene)-2-butenylidene]-1,3-diethyl-2-thiobarbituric acid (n.c., H); 151. 5-[(3-ethyl-2(3H)-benzothiazolylidene)-2-butenylidene]-1-ethyl-3-( $\beta$ -diemthyl-amino ethyl hydrobromide)-barbituric acid (n.c., M); 152. 5-[(3-ethyl-2(3H)-benzothiazolylidene)-ethylidene]-3-phenyl-2-thiobarbituric acid (n.c., M); 153. 5-[(3-ethyl-2(3H)-thiazolylidene)-2-butenylidene]-1,3-dibutyl-2-thiobarbituric acid (1.0, H); 154. 5-[(3-ethyl-2(3H)-thiazolylidene)-2,4-hexadienylidene]-1,3-diethyl-2-thiobarbituric acid (0.9, H); 155. 5-[(1- $\gamma$ -sodium-sulfopropyl-2(3H)-quinolylidene)-2-butenylidene]-1,3-diethyl-2-thiobarbituric acid (n.c., H); 156. 4-[(1- $\beta$ -carboxyethyl-4(1H)-quinolylidene)-ethylidene]-3-methyl-1-phenyl-5-pyrazolone (n.c., NK 1288). 157. 4-[(1-ethyl-4(1H)-quinolylidene)-ethylidene]-3-methyl-1-*p*-sulfophenyl-5-pyrazolone (n.c., NK 1286); 158. 5-[(3- $\gamma$ -sodium-sulfopropyl-2(3H)-benzoxazolylidene)-2-butenylidene]-4-cyano-3-phenyl-2-oxo-oxolane (0.08, M); 159. 4-[(3- $\beta$ -carboxyethyl-2(3H)-benzothiazolylidene)-ethylidene]-1,3-diethyl-2-thiohydantoin (n.c., NK 1245); 160. 5-[(3-ethyl-2(3H)-benzoxazolylidene)-ethylidene]-1,3-diphenyl-2-thiohydantoin (n.c., NK 1074); 161. 4-[(1,3,3-trimethyl-2(3H)-indolylidene)-ethylidene]-3-phenyl-5(4H)-isoxazolone (n.c., NK 1436); 162. 2-[(3-ethyl-2(3H)-benzothiazolylidene)-ethylidene]-3(2H)-thianaphthenone (n.c., NK 1584); 163. 2-[(3-ethyl-2(3H)-benzothiazolylidene)-2-butenylidene]-3(2H)-thianaphthenone (n.c., NK 1585); 164. 4-[(1-carboxymethyl-4(1H)-pyridylidene)-2,4-hexadienylidene]-3-phenyl-5(4H)-isoxazolone (0.06, M); 165. 4-[(1-methyl-4(1H)-pyridylidene)-2,4-hexadienylidene]-3-phenyl-5(4H)-isoxazolone (0.05, Y); 166. quinoline yellow (n.c., D); 167. 5-anilinomethylene-1,3-diethyl-2-thiohydantoin (n.c., NK 1250); 168. orthochrome T (0.06, M); 169. 3,5-bis-[(5,6-benzo-3-methyl-2(3H)-benzoxazolylidene)-ethylidene]-2,4,6-trioxo-oxane (n.c., M); 170. 5-[(3-ethyl-2(3H)-benzoxazolylidene)-1,3-neopentylene-2,4-hexadienylidene]-1,3-diethylbarbituric acid (0.4, M); 171. 5-[5-(2,3,6,7-tetrahydro-4H,5H-benzo [i,j]-quinolizin-9-yl)-1,3-neopentylene-2,4-pentadienylidene]-1,3-diethyl-2-thiobarbituric acid (n.c., M).

#### Merocyanine Rhodanine Dyes

172. 5-[(1,3,3-trimethyl-2(3H)-indolylidene)-ethylidene]-3-ethyl-2-thio-2,4-oxazolidine-dione (n.c., NK 1474); 173. 5-[(3,3-dimethyl-1- $\gamma$ -sodium-sulfopropyl-2(3H)-indolylidene)-2-butenylidene]-3-ethyl rhodanine (0.5, H); 174. 5-[(3,3-dimethyl-1-propyl-2(3H)-indolylidene)-2-butenylidene]-3-ethyl rhodanine (n.c., H); 175. 5-[(1,3,3-trimethyl-2(3H)-indolylidene)-2-butenylidene]-3-ethyl rhodanine (2.0, NK 1269); 176. 5-[(3-ethyl-2(3H)-benzoxazolylidene)-ethylidene]-3-ethyl rhodanine (n.c., NK 1249); 177. 5-[(3-ethyl-2(3H)-benzoxazolylidene)-ethylidene]-3-allyl rhodanine (n.c., NK 1141); 178. 5-[(1-ethyl-4(1H)-quinolylidene)-ethylidene]-3-carboxymethyl rhodanine (n.c., NK 1663); 179. 5-[(1-ethyl-2(1H)-quinolylidene)-2-butenylidene]-3-ethyl rhodanine (n.c., NK 1319); 180. 5-[(1-ethyl-2(1H)-quinolylidene)-ethylidene]-3-ethyl rhodanine (n.c., NK 1218); 181. 5-[(3- $\beta$ -carboxyethyl-2(3H)-benzothiazolylidene)-ethylidene]-3-ethyl rhodanine (0.02, NK 1149); 182. 5-[(3,4-dimethyl-5-carboxy-2(3H)-thiazolylidene)-ethylidene]-3-ethyl rhodanine (0.01, NK 1463); 183. 5-[(3-ethyl-4-methyl-5-carbethoxy-2(3H)-2-thiazolylidene)-ethylidene]-3-carboxy rhodanine (0.01, NK 1460).

#### Rhodacyanine Dyes

184. 5-[(1-ethyl-4(1H)-quinolylidene)-ethylidene]-2-[(7-isopropyl-2-benzoxazolyl methiodide)-methylene]-3-ethyl-4-oxo-thiazolidine (n.c., NK 1716); 185. 5-[(3-ethyl-2(3H)-benzoxazolylidene)-ethylidene]-2-[(4-methyl-2-oxazolyl ethiodide)-methylene]-3-ethyl-4-oxo-thiazolidine (0.2, NK 1423); 186. 5-[(1,3,3-trimethyl-2(3H)-indolylidene)-ethylidene]-2-[(4,5-diphenyl-2-thiazolyl ethiodide)-methylene]-3-ethyl-4-oxo-thiazolidine (0.6, NK 1421).

## Oxonol Dyes

187. Bis-[1-octyl-3-carboxymethyl-barbituric acid-(5)]-pentamethinoxonol (0.8, M); 188. Bis-[3-ethyl rhodanine-(5)]-trimethinoxonol (0.1, NK 1451); 189. Bis-[3-phenyl rhodanine-(5)]-pentamethinoxonol (n.c., NK 1747); 190. Bis-[3(2H)-thianaphthenone-(2)]-methinoxonol (0.3, NK 1128); 191. Bis-[3-methyl-1-phenyl-5-pyrazolone-(4)]-trimethinoxonol (0.04, NK 1445); 192. Bis-[3-methyl-1-phenyl-5-pyrazolone-(4)]-methinoxonol (n.c., NK 1743); 193. Bis-[1,3-diethylbarbituric acid-(5)]-pentamethinoxonol (0.75, M).

## Styryl Dyes

194. 2-(*p*-dimethylaminostyryl)-1-ethyl-quinolinium iodide (quinaldine red) (0.4, C, NK 383); 195. 2-(*p*-dimethylaminostyryl)-1-hexyl-quinolinium iodide (0.1, H); 196. 2-(*p*-dimethylaminostyryl)-1-octyl-quinolinium iodide (0.15, H); 197. 2-(*p*-dimethylaminostyryl)-1-decyl-quinolinium iodide (0.1, H); 198. 2-(*p*-dimethylaminostyryl)-1-dodecyl-quinolinium iodide (n.c., H); 199. 2-(*p*-dimethylaminostyryl)-1-hexadecyl-quinolinium iodide (n.c., H); 200. 2-(*p*-dimethylaminostyryl)-1-( $\beta$ -carboxyethyl)-quinolinium iodide (n.c., NK 1406); 201. 2,4-di-(*p*-dimethylaminostyryl)-1-ethyl-quinolinium iodide (0.05, NK 333); 202. 2-(*p*-hydroxystyryl)-1-ethyl-6-dimethylamino-quinolinium iodide (0.02, NK 1653); 203. 2-(*p*-dimethylaminostyryl)-1-ethyl-6-dimethylamino-quinolinium iodide (0.5, NK 458); 204. 2-[ $\beta$ -(2-pyridyl methiodide)-vinyl]-1-methyl-quinolinium iodide (n.c., NK 906); 205. 2-[ $\beta$ -(2-pyridyl)-vinyl]-1-methyl-quinolinium iodide (n.c., NK 905); 206. 2-[ $\beta$ -(5-benzo[d]-1,3-dioxolanyl)-vinyl]-1-ethyl-quinolinium iodide (n.c., NK 591); 207. 4-(*p*-dimethylaminostyryl)-1-ethyl-quinolinium iodide (1.0, NK 96); 208. 4-[4-(*p*-dimethylaminophenyl)-1,3-butadienyl]-1-ethylquinolinium iodide (1.6, NK 526); 209. 4-[*p*-dimethylaminostyryl]-1-heptyl-quinolinium iodide (1.8, NK 232); 210. 4-(*p*-dimethylaminostyryl)-1-( $\beta$ - $\gamma$ -dihydroxypropyl)-quinolinium iodide (0.4, NK 602); 211. 2-(*p*-dimethylaminostyryl)-pyridine (n.c., NK 1341); 212. 2-(*p*-dimethylaminostyryl)-1-methyl-pyridinium iodide (n.c., NK 99); 213. 2-(*p*-dimethylaminostyryl)-1-butyl-pyridinium iodide (0.03, NK 313); 214. 2-[4-(*p*-dimethylaminophenyl)-1,3-butadienyl]-1-butyl-pyridinium iodide (0.3, NK 401); 215. 4-(*p*-dimethylaminostyryl)-1-allyl-pyridinium iodide (n.c., NK 895); 216. 4-(*p*-dimethylamino- $\alpha$ -methylstyryl)-1-methyl-pyridinium iodide (n.c., NK 671); 217. 4-[4-(*p*-dimethylaminophenyl)-1,3-butadienyl]-1-methyl-pyridinium iodide (0.07, NK 361); 218. 2-[4-(*p*-dimethylaminophenyl)-1,3-butadienyl]-1,3,3-trimethyl-pseudindolium iodide (0.5, NK 377); 219. basic violet 16 (0.1, P, NK 97); 220. astrazone red 6B (n.c., D); 221. astrazone yellow 3G (n.c., O, D); 222. astrazone red (1.1, E); 223. 2-(*p*-dimethylaminostyryl)-3-propyl-benzothiazolium iodide (n.c., H); 224. 2-(*p*-dimethylaminostyryl)-3-decyl-benzothiazolium iodide (n.c., H); 225. anhydro-2-(*p*-dimethylaminostyryl)-3-( $\gamma$ -sulfopropyl)-benzothiazolium hydroxide (0.3, H); 226. 2-(*p*-dimethylaminostyryl)-3,4-dimethyl-thiazolium iodide (n.c., NK 90); 227. 2-(*p*-dimethylaminostyryl)-4-isobutyl-3,5-dimethyl-thiazolium iodide (0.03, NK 1025); 228. 2-[ $\beta$ -(3-pyridyl ethiodide)-vinyl]-3,4-dimethyl-thiazolium iodide (n.c., NK 911); 229. 2-(*p*-dimethylaminostyryl)-1-propyl-benzoxazolium iodide (0.15, H); 230. anhydro-2-(*p*-dimethylaminostyryl)-3-( $\gamma$ -sulfopropyl)-benzoxazolium hydroxide (n.c., H); 231. 2-(*p*-hydroxystyryl)-3-ethyl-5,6-dimethyl-benzoxazolium iodide (n.c., NK 1645); 232. 2-(*p*-dimethylaminostyryl)-3,4-dimethyl-oxazolium iodide (n.c., NK 548); 233. 2-(*p*-hydroxystyryl)-3,4,5-trimethyl-oxazolium iodide (n.c., NK 991); 234. 2-(*p*-dimethylaminostyryl)-3-methyl-4,5-diphenyl-oxazolium iodide (0.4, NK 1600); 235. 2-[4-(*p*-dimethylaminophenyl)-1,3-butadienyl]-3,5-dimethyl-oxazolium iodide (n.c., NK 929); 236. 2-[4-(*p*-dimethylaminophenyl)-1,3-butadienyl]-1,3-dimethyl-benzimidazolium iodide (0.03, NK 360); 237. 5-(3-*p*-dimethylaminophenyl-2-propenylidene)-1,3-bis-( $\beta$ -diethylaminoethyl hydrochloride)-barbituric acid (0.4, M); 238. 4-(*p*-dimethyl-



aminobenzylidene)-3-methyl-1-phenyl-5-pyrazolone (n.c., NK 1107); 239. 4- $[\beta$ -(2-furyl)-vinyl]-1-methyl-pyridinium iodide (n.c., NK 841); 240. 2- $[(1\text{-ethyl-quinolyldiene})\text{-1-propenyl}]\text{-1-ethyl-6-}(p\text{-dimethylaminostyryl})\text{-pyridinium iodide}$  (n.c., NK 336).

#### Amino Vinyl Dyes

241. 2-(2-*p*-dimethylaminoanilinovinyl)-1,3,3-trimethyl-pseudindolium iodide (n.c., NK 531); 242. 4-(2-*p*-dimethylaminoanilinovinyl)-1-ethyl-quinolinium iodide (n.c., NK 495); 243. 2-(2-*p*-dimethylaminoanilinovinyl)-1-pentyl-6-methyl-pyridinium iodide (n.c., NK 1675); 244. 2-(2-*p*-dimethylaminoanilinovinyl)-1-ethyl-6-dimethylamino-quinolinium iodide (n.c., NK 552); 245. 2-(2-*p*-dimethylaminoanilinovinyl)-3,4-dimethyl-oxazolium iodide (n.c., NK 1608).

#### Harmine Compounds

246. harmine HCl (0.04, R); 247. harmane 1,2,3,4-tetrahydro-3-carboxylic acid (n.c., R); 248. harmol (n.c., R); 249. harminic acid (n.c., R); 250. harmalol (n.c., R); 251. harmane HCl (0.02, R).

#### Other Structural Types

252. 6-(9-anthroyl)-hexyl triethyl ammonium iodide (anthroyl-TEA-6C) (0.008, H); tetracycline (0.01, T); 254. chlorotetracycline (0.006, T); 255. auramine O (0.01, B); 256. ethidium bromide (0.003, K); 257. intrawite WGS (0.03, O); 258. intrawite CF (0.06, O); 259. intrawite EBF (c.n., O); 260. alcian blue 8GS (n.c., A); 261. alizarin red S (n.c., A); 262. amiloride (n.c., S); 263. aurantia (n.c., A); 264. berberine sulfate (n.c., A); 265. brilliant sulfoflavine (n.c., A, E); 266. chlorophyll (n.c., A); 267. 1-butyl-6-hydroxy-quinolinium iodide (n.c., H); 268. indigo carmine (n.c., A); 269. martius yellow (n.c., A); 270. morin (n.c., A); 271. orcein (n.c., A); 272. 1-pyrenebutyric acid (n.c., M); 273. saffron (n.c., A); 274. soledon yellow G (n.c., W); 275. tetrazolium blue (n.c., A); 276. basic yellow 13 (n.c., P); 277. basic yellow 23 (n.c., P); 278. basic yellow 25 (n.c., P); 279. rhubarb extract (n.c., E); 280. 1-anilino-8-naphthalene sulfonate (ANS) (0.2, F); 281. N-octadecyl naphthyl-2-amine-6-sulfonate (ONS) (0.005, H).

### References

- Armstrong, C. M., Binstock, L. 1965. Anomalous rectification in the squid giant axon injected with tetraethylammonium chloride. *J. Gen. Physiol.* **48**:859
- Arvanitaki, A., Chalazonitis, N. 1961. Excitatory and inhibitory processes initiated by light and infra-red radiations in single excitable nerve cells (giant ganglion cells of *Aplysia*). In: *Nervous Inhibition*. E. Florey, editor. p. 194. Pergamon Press, New York
- Baker, P. F., Hodgkin, A. L., Ridgway, E. B. 1971. Depolarization and calcium entry in squid giant axons. *J. Physiol., Lond.* **218**:709
- Bezanilla, F., Horowicz, P. 1974. Fluorescence changes in frog muscle stained with Nile blue associated with excitation-contraction coupling. *Fed. Proc.* **33**:1259
- Beyer, C. F., Craig, L. C., Gibbons, W. A. 1973. Structural requirements for binding and fluorescence enhancement of the fluorescent probe TNS with peptides. *Nature, New Biol.* **241**:78
- Braddick, H. J. J. 1960. Photoelectric photometry. *Prog. Phys.* **23**:154
- Brooker, L. G. S., Keyes, G. H., Sprague, R. H., Van Dyke, R. H., Van Lare, E., Van Zandt, G., White, F. L., Cressman, H. W. J., Dent, S. G., Jr. 1951. Color and constitution. X. Absorption of the merocyanines. *J. Amer. Chem. Soc.* **73**:5332

- Bücher, H., Wiegand, J., Snavely, B. B., Beck, K. H., Kuhn, H. 1969. Electric field induced changes in the optical absorption of a merocyanine dye. *Chem. Phys. Lett.* **3**:508
- Camejo, G., Villegas, G. M., Barnola, F. V., Villegas, R. 1969. Characterization of two different membrane fractions isolated from the first stellar nerves of the squid, *Dosidicus gigas*. *Biochim. Biophys. Acta* **193**:247
- Caswell, A. H., Hutchison, J. D. 1971. Visualization of membrane bound cations by a fluorescent technique. *Biochem. Biophys. Res. Commun.* **42**:43
- Chance, B. 1973. Electrochromic responses of merocyanine probes in energy coupling responses of submitochondrial particles (SMP). *Fed. Proc.* **32**:669 (abs.)
- Cohen, L. B. 1973. Changes in neuron structure during action potential propagation and synaptic transmission. *Physiol. Rev.* **53**:373
- Cohen, L. B., Davila, H. V., Waggoner, A. S. 1971. Changes in axon fluorescence. *Biol. Bull., Woods Hole* **141**:382 (Abstr.)
- Cohen, L. B., Hille, B., Keynes, R. D. 1969. Light scattering and birefringence changes during activity in the electric organ of *Electrophorus electricus*. *J. Physiol., Lond.* **203**:489
- Cohen, L. B., Hille, B., Keynes, R. D., Landowne, D., Rojas, E. 1971. Analysis of the potential-dependent changes in optical retardation in the squid giant axon. *J. Physiol., Lond.* **218**:205
- Cohen, L. B., Keynes, R. D., Landowne, D. 1972a. Changes in light scattering that accompany the action potential in squid giant axons: Potential-dependent components. *J. Physiol., Lond.* **224**:701
- Cohen, L. B., Keynes, R. D., Landowne, D. 1972b. Changes in axon light scattering that accompany the action potential: Current-dependent components. *J. Physiol., Lond.* **224**:727
- Cohen, L. B., Landowne, D., Shrivastav, B., Ritchie, J. M. 1970. Changes in fluorescence of squid axons during activity. *Biol. Bull., Woods Hole* **139**:418 (abs.)
- Cohen, L. B., Salzberg, B. M., Davila, H. V. 1973. Changes in fluorescence of a squid giant axon during excitation, a demonstration. *Biol. Bull., Woods Hole* **145**:429 (abs.)
- Cole, K. S., Curtis, H. J. 1939. Electrical impedance of the squid giant axon during activity. *J. Gen. Physiol.* **22**:649
- Colour Index, 3rd ed., 1971. Society of Dyers and Colourists and American Association of Textile Chemists and Colorists
- Colquhoun, D., Henderson, R., Ritchie, J. M. 1972. The binding of labeled tetrodotoxin to non-myelinated nerve fibres. *J. Physiol., Lond.* **227**:95
- Conti, F., Tasaki, I. 1970. Changes in extrinsic fluorescence in squid axons during voltage-clamp. *Science* **169**:1322
- Conti, F., Tasaki, I., Wanke, E. 1971. Fluorescence signals in ANS-stained squid giant axons during voltage clamp. *Biophysik* **8**:58
- Czikkely, V., Dreizler, G., Försterling, H. D., Kuhn, H., Sondermann, J., Tillmann, P., Wiegand, J. 1969. Lichtabsorption von Farbstoff-Molekülpaaen in Sandwichsystemen aus monomolekularen Schichten. *Z. Naturf.* **249**:1821
- Davila, H. V., Cohen, L. B., Salzberg, B. M., Shrivastav, B. B. 1974. Changes in ANS and TNS fluorescence in giant axons from *Loligo*. *J. Membrane Biol.* **15**:29
- Davila, H. V., Salzberg, B. M., Cohen, L. B., Waggoner, A. S. 1973. A large change in axon fluorescence that provides a promising method for measuring membrane potential. *Nature, New Biol.* **241**:159
- Dobres, H. L., Moats, W. A. 1968. Qualitative analysis by thin layer chromatography of some common dyes used in biological staining. *Stain Tech.* **43**:27
- Dunnigan, M. G. 1968. Chromatographic separation and photometric analysis of the components of Nile blue sulphate. *Stain Tech.* **43**:243

- Emrich, H. M., Junge, W., Witt, H. T. 1969. An artificial indicator for electric phenomena in biological membranes and interfaces. *Naturwissenschaften* **56**:514
- Furusawa, K. 1929. The depolarization of crustacean nerve by stimulation or oxygen want. *J. Physiol., Lond.* **67**:325
- Goldring, J. M., Blaustein, M. P. 1973. Synaptosome membrane potential changes monitored with a fluorescent probe. Paper presented at the third annual meeting, Society for Neuroscience, San Diego, California
- Hallett, M., Schneider, A. S., Carbone, E. 1972. Tetracycline fluorescence as calcium-probe for nerve membrane with some model studies using erythrocyte ghosts. *J. Membrane Biol.* **10**:31
- Hamer, F. M. 1964. The Cyanine Dyes and Related Compounds. John Wiley & Sons, New York
- Hodgkin, A. L., Huxley, A. F. 1952. A quantitative description of membrane current and its application to conduction and excitation in nerve. *J. Physiol., Lond.* **117**:500
- Hodgkin, A. L., Keynes, R. D. 1957. Movement of labelled calcium in squid giant axons. *J. Physiol., Lond.* **138**:253
- Hoffman, J. F., Laris, P. C. 1974. Determination of membrane potentials in human and amphiuma red blood cells using a fluorescent probe. *J. Physiol., Lond.* **239**:519
- Keynes, R. D. 1963. Chloride in the squid giant axon. *J. Physiol., Lond.* **169**:690
- Landowne, D. 1974. Changes in fluorescence of skeletal muscle stained with merocyanine associated with excitation-contraction coupling. *J. Gen. Physiol. (In press)*
- Levin, S. V., Rozenthal, D. L., Komissarchik, Y. Y. 1968. Structure changes in the axon membrane on excitation. *Biofizika* **13**:180
- Lillie, R. D. 1969. H. J. Conn's Biological Stains, 8th Ed. Williams & Wilkins, Baltimore
- Löhr, W., Wittekind, D. 1973. Vitalfärbung mit Derivaten des Phenothiazins. *Z. Zellforsch.* **137**:125
- Malley, M., Feher, G., Mauzerall, D. 1968. The Stark effect in porphyrins. *J. Mol. Spectroscopy* **25**:544
- Moore, J. W., Narahashi, T., Shaw, T. I. 1967. An upper limit to the number of sodium channels in nerve membrane? *J. Physiol., Lond.* **188**:99
- Muralt, A. von. 1971. "Optical spike" during excitation in peripheral nerve. *Abstr. 25th Int. Physiol. Congr., Munich.* p. 638
- Nasonov, D. N. 1962. Local Reaction of Protoplasm and Gradual Excitation. Akademiya Nauk SSSR, Moscow-Leningrad. (Translated by the Israel Program for Scientific Translations, Jerusalem.)
- Platt, J. R. 1962. Electrochromism, a possible change of color producible in dyes by an electric field. *J. Chem. Phys.* **34**:862
- Pooler, J. 1972. Photodynamic alteration of sodium currents in lobster axons. *J. Gen. Physiol.* **60**:367
- Salzberg, B. M., Davila, H. V., Cohen, L. B. 1973. Optical recording of impulses in individual neurons of an invertebrate central nervous system. *Nature* **246**:508
- Salzberg, B. M., Davila, H. V., Cohen, L. B., Waggoner, A. S. 1972. A large change in axon fluorescence, potentially useful in the study of simple nervous systems. *Biol. Bull., Woods Hole* **143**:475 (abs.)
- Sims, P. J., Wang, C. H., Waggoner, A. S., Hoffman, J. F. 1974. The cyanine dyes as probes of membrane potential. *Biochemistry* **13**:3315
- Tasaki, I., Carnay, L., Watanabe, A. 1969. Transient changes in extrinsic fluorescence of nerve produced by electric stimulation. *Proc. Nat. Acad. Sci.* **64**:1362

- Tasaki, I., Watanabe, A., Hallett, M. 1972. Fluorescence of squid axon membrane labelled with hydrophobic probes. *J. Membrane Biol.* **8**:109
- Villegas, G. M. 1969. Electron microscopic study of the giant nerve fiber of the giant squid *Dosidicus gigas*. *J. Ultrastruct. Res.* **26**:501
- West, W., Pearce, S. 1965. The dimeric state of cyanine dyes. *J. Phys. Chem.* **69**:1894